Journal of Medicinal Chemistry

Article

Design, Synthesis, and Pharmacological Characterization of N-(4-(2 (6,7-dimethoxy-3,4-dihydroisoquinolin-2(1H)yl)ethyl)phenyl) quinazolin-4-amine Derivatives: Novel Inhibitors Reversing P-glycoprotein-Mediated Multidrug Resistance

Qianqian Qiu, Baomin Liu, Jian Cui, Zheng Li, Xin Deng, Hao Qiang, Jieming Li, Chen Liao, Bo Zhang, Wei Shi, Miaobo Pan, Wenlong Huang, and Hai Qian

J. Med. Chem., **Just Accepted Manuscript** • DOI: 10.1021/acs.jmedchem.6b01787 • Publication Date (Web): 29 Mar 2017

Design, Synthesis, and Pharmacological Characterization of *N*-(4-(2 (6,7-dimethoxy-3,4-dihydroisoquinolin-2(1*H*)yl)ethyl)phenyl) quinazolin-4-amine Derivatives: Novel Inhibitors Reversing P-glycoprotein-Mediated Multidrug Resistance

Qianqian Qiu[a,#], Baomin Liu[a,#], Jian Cui[a], Zheng Li[a], Xin Deng[a], Hao Qiang[a], Jieming Li[a], Chen Liao[a], Bo Zhang[a], Wei Shi[a], Miaobo Pan[a], Wenlong Huang [a,b,*] and Hai Qian [a,b,*]

[a] Center of Drug Discovery, State Key Laboratory of Natural Medicines, China Pharmaceutical University, Nanjing, PR China

[b] Jiangsu Key Laboratory of Drug Discovery for Metabolic Disease, China Pharmaceutical University, Nanjing, PR China

ABSTRACT

P-glycoprotein (P-gp)-mediated multidrug resistance (MDR) is a principal obstacle for successful cancer chemotherapy. A novel P-gp inhibitor with a quinazoline scaffold, **12k,** was considered to be the most promising for in-depth study. **12k** possessed high potency (EC_{50} = 57.9 ± 3.5 nM), low cytotoxicity and long duration of activity in reversing doxorubicin (DOX) resistance in K562/A02 cells. **12k** also boosted the potency of other MDR-related cytotoxic agents with different structures, increased accumulation of DOX, blocked P-gp-mediated Rh123 efflux, and suppressed P-gp ATPase activity in K562/A02 MDR cells. However, **12k** did not have any effects on CYP3A4 activity or P-gp expression. In particular, **12k** had a good half-life and oral bioavailability, and displayed no influence on DOX metabolism to obviate the side-effects closely related to increased plasma concentrations of cytotoxic agents *in vivo*.

KEYWORDS: P-glycoprotein; multidrug resistance; quinazoline; reversal activity

INTRODUCTION

The development of multidrug resistance (MDR) to anticancer drugs is a leading cause of failure for cancer treatment.[1-3] Mechanisms involved in MDR have been characterized extensively and shown to be quite complicated. Overexpression of P-glycoprotein (P-gp) is the most common mechanism of MDR.[4, 5] P-gp, also known as adenosine triphosphate (ATP) binding-cassette subfamily B member 1 (ABCB1), is encoded by MDR1 gene and extrudes various cytotoxic agents out of cells by the energy of adenosine triphosphate (ATP) hydrolysis, resulting in low and ineffective intracellular drug concentrations and MDR to cancer cells.[6, 7]

Co-administration of P-gp modulators with anticancer drugs in the clinic has long been recognized as a promising strategy to circumvent P-gp-mediated MDR, and considerable efforts have been made to develop three generations of P-gp inhibitors over the past few decades.[8] In particular, third-generation P-gp inhibitors comprise compounds such as WK-X-34 (**1**), HM30181 (**2**) and tariquidar (XR9576, **3**) with high affinity to P-gp at a nanomolar concentration to acquire inhibition of P-gp function specifically and effectively (**Figure 1A**).[9-11] 6,7-dimethoxy-2-phenethyl-1,2,3,4-tetrahydro-isoquinoline is the most characteristic structure in these excellent inhibitors, and has been considered to be the foremost active domain to have an efficient role in P-gp inhibition.[12, 13] However, a P-gp inhibitor has not been approved for the market due to a lack of significant clinical efficacy, pharmacokinetic interaction or concerns about its safety.[14] Therefore, there is an urgent need to develop new agents to overcome MDR.[15, 16]

The quinazoline core, as a crucial aromatic heterocycle, is commonly present in various tyrosine kinase inhibitors (TKIs), including gefitinib (**4**), lapatinib (**5**) and erlotinib (**6**), which have been identified as substrates or modulators of P-gp and other ABC transporters (**Figure 1B**).[17-19] In addition, some pre-clinical studies and clinical trials are underway to evaluate the co-administration of anticancer drugs with these TKIs to conquer drug resistance and improve therapeutic outcome in cancer patients. Quinazoline is thought to interact with the active region of P-gp, and 4-anilino-quinazolines have been reported to be inhibitors of breast cancer resistance protein.[20] Extensive efforts have been devoted to develop further bioactive molecules on the basis of quinazoline fragment. Structural modifications of promising P-gp inhibitors by introduction of

quinazoline scaffolds is a convenient and rewarding method to exploit new P-gp reversal agents with strong bioactivity, outstanding affinity to P-gp targets and high safety profile.

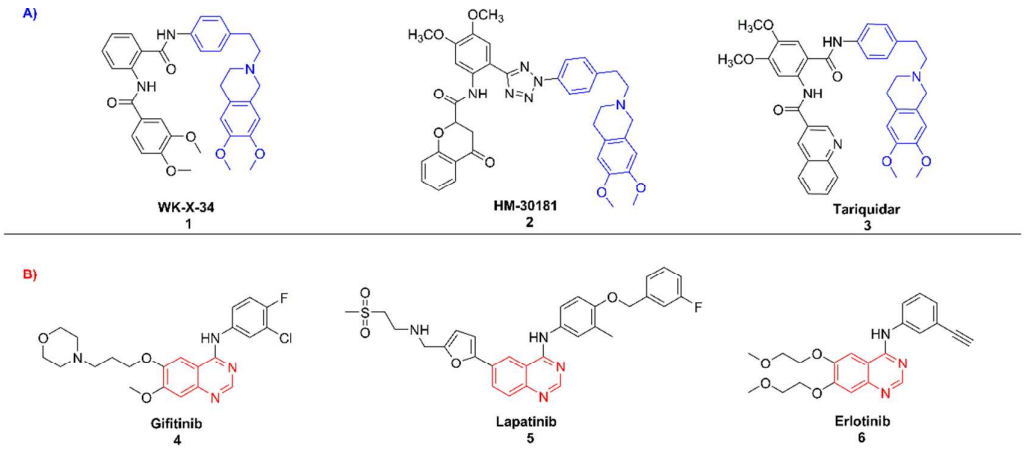

Figure 1. A) Selected P-gp inhibitors; **B**) TKIs with P-gp inhibitory activity

In the present study, we designed and synthesized a series of 2-arylquinazolines containing the group 6,7-dimethoxy-2-phenethyl-1,2,3,4-tetrahydro-isoquinoline (**12a–s**) *via* substitution (**Figure 2**). Then, we evaluated their effects on cell viability and MDR reversal activity in cells sensitive or resistant to DOX. After preliminary biological evaluations, compound **12k,** which showed the most potency, was investigated further with regard to its potency and mechanism of reversing P-gp-mediated drug resistance.

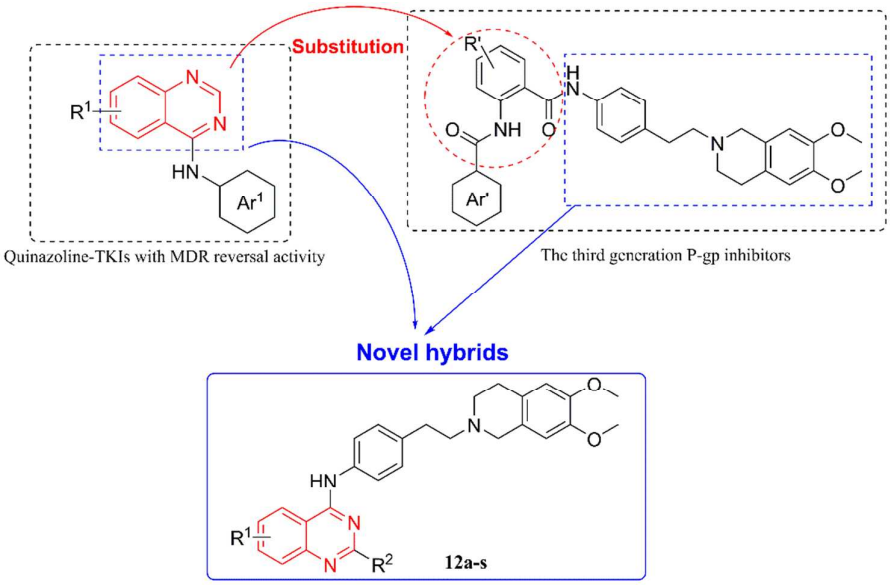

Figure 2. Design of novel target compounds

RESULTS AND DISCUSSION

Chemistry

The intermediate **7a–s** was readily prepared by the reaction of commercial substituted 2-aminobenzoic acid and aromatic acyl chloride. The synthesized **7a–s** was heated in NH_4OH/EtOH at 80°C for 12 h to afford quinazolin-4(3*H*)-ones **8a–s**, which were then reacted with 10 eq. $SOCl_2$ at 50°C for 6 h to produce the desired intermediate **9a–s**. Under reflux conditions, commercial 6,7-dimethoxy-1,2,3,4-tetrahydroisoquinoline hydrochloride and 1-(2-bromoethyl)-4-nitrobenzene were reacted for 17 h to produce compound **10**. Then, reduction of compound **10** under hydrogen atmosphere with Pd/C as catalyst delivered compound **11**. Further nucleophilic reaction of compounds **9a–s** and **11** gave target compounds **12a–s**. Structures of all target compounds are presented in **Table 1**. All structures of the new compounds were confirmed by ^{1}H NMR, ^{13}C NMR, HRMS and IR spectra. Moreover, the purity of target compounds **12a–s** was ascertained by ultra high performance liquid chromatography (UHPLC). Results demonstrated that all compounds had a purity of ≥ 95% (Experimental Section).

Scheme 1. Synthesis of target compounds **12a-s**[a]

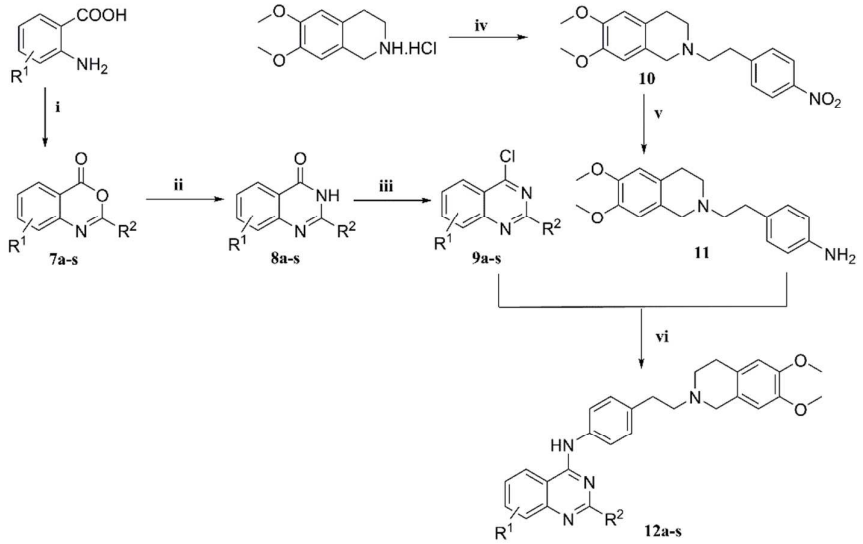

[a] Reagents and conditions: (i) R_2COCl, pyridine, r.t., 6 h; (ii) NH_4OH/EtOH, 80°C, 12 h; (iii) 10 eq. $SOCl_2$, 50°C, 6 h; (iv) 1-(2-bromoethyl)-4-nitrobenzene, K_2CO_3, CH_3CN, reflux, 17 h; (v) H_2, Pd/C, EtOH/CH_2Cl_2, r.t., 24 h; (vi) CH_3SO_3H, EtOH, reflux.

Table 1 Structures of target compounds

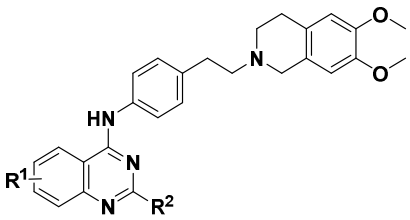

compound	R^1	R^2	compound	R^1	R^2
12a	H	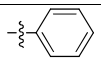	**12k**	H	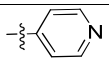
12b	H	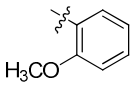	**12l**	H	
12c	H	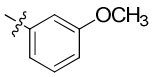	**12m**	H	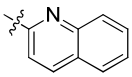
12d	H	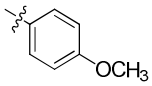	**12n**	H	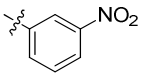
12e	H	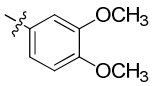	**12o**	H	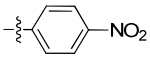
12f	H	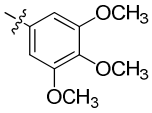	**12p**	H	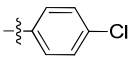
12g	H	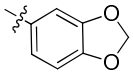	**12q**	H	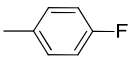
12h	H	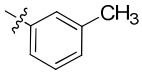	**12r**	7-Cl	
12i	H	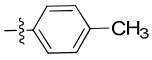	**12s**	6,7-diOCH_3	

12j	H	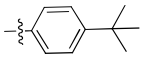

Biological evaluation

Effects of target compounds on cell viability

Before evaluation of MDR reversal potency, the effects of these compounds at 1.0 μM on the viability of sensitive K562 cells and its DOX-resistant K562/A02 cells with overexpressed P-gp were determined preliminarily by the MTT assay. Anticancer drug DOX and P-gp inhibitor verapamil (VRP) were served as controls. As present in **Table 2**, 19 target compounds showed hardly any toxicity toward these two cell lines. Survival of K562 cells using 5.0 μM DOX was only 8.8%, whereas toxicity of 5.0 μM DOX towards K562/A02 cells was inferior to 4 %.

Table 2 Survival rate of target compounds at 1.0 μM toward K562 and K562/A02 cell (%) [a]

Compound	K562	K562/A02	Compound	K562	K562/A02
12a	98.7 ± 1.5	> 99.0	**12m**	> 99.0	92.1 ± 1.5
12b	> 99.0	> 99.0	**12n**	> 99.0	> 99.0
12c	> 99.0	> 99.0	**12o**	94.7 ± 2.1	> 99.0
12d	> 99.0	85.2 ± 0.8	**12p**	> 99.0	> 99.0
12e	95.1 ± 1.6	> 99.0	**12q**	> 99.0	> 99.0
12f	> 99.0	96.5 ± 2.1	**12r**	> 99.0	95.3 ± 1.3
12g	91.4 ± 3.0	89.2 ± 4.2	**12s**	> 99.0	97.3 ± 3.2
12h	92.9 ± 1.8	92.1 ± 2.2	**1**	97.5 ± 3.0	> 99.0
12i	93.4 ± 0.5	94.2 ± 1.3	5.0 μM VRP	> 99.0	88.3 ± 5.1
12j	> 99.0	91.3 ± 1.0	5.0 μM DOX	8.8 ± 1.1	96.4 ± 3.2

12k	96.5 ± 2.2	> 99.0	Control [b]	> 99.0	> 99.0
12l	> 99.0	97.9 ± 0.7			

[a] Survival rates of target compounds toward cells were determined by MTT assay and data are presented as mean ± SD for three independent tests. [b] 0.1% DMSO was used as solvent control.

Reversal of DOX resistance

Based on survival results, a concentration of 1.0 μM was used to investigate the effects of 19 target compounds on reversal of resistance to DOX in K562/A02 cells. Data on the reversal activity of all compounds are depicted in **Table 3**. DOX alone demonstrated little toxic effect on K562/A02 cells (half-maximal inhibitory concentration IC_{50} = 89.8 ± 4.52 μM). However, co-administration of DOX and target compounds or VRP led to an increase of toxic effects on K562/A02 cells to different extents, suggesting that all test compounds could reverse resistance to DOX.

First, **12a** with unsubstituted phenyl increased reversal activity considerably from 4.2-reversal fold (RF) of the positive control VRP to 7.7-RF. The *para* position-substituted compounds **12d, i, j, o, p** and **q**, irrespective of whether they had an electron-withdrawing or -donating group, displayed similar or lower reversal activity compared with **12a**. In particular, **12j, o** and **q** were inferior to VRP. Interestingly, the *ortho* and *meta* position-substituted **12b, c, h** and **n** exhibited increased activity at different extents. Furthermore, the effects of multiple substitution with methoxy groups at the phenyl moiety were investigated. Results suggested that disubstitution with methoxy groups contributed greatly to the increase in reversal activity (**12e**, and **g**), whereas a positive effect was not observed from trisubstitution with methoxy groups (**12f**), perhaps due to steric hindrance. To explore this reversal activity further, we synthesized compounds containing R^2 replaced with nitrogen heterocycles and R^1 substituted with electron-withdrawing or -donating groups, most of which exhibited no or minor benefit to reversal activity (**12l, m, r** and **s**), except **12k**. Surprisingly, 1.0 μM **12k** presented more remarkable MDR reversal activity than 5.0 μM VRP, with much higher RF than **1**.

Some factors related to the activity of a substance can be derived from these results. The electronic effect (electron-withdrawing and electron-donating) of the substituents at the phenyl moiety as well as steric requirements plays a minor part. Substitution at *meta* and *ortho* positions yielded high activities. However, a distinct advantage for disubstitution with methoxy substituents was found, whereas trisubstitution was a disadvantage. Simultaneously, a quinazoline moiety with an electron-withdrawing (R^1 = 7-Cl) or -donating (R^1 = 6,7-diOCH_3) group had little effect. Also, nitrogen heterocycles made a distinct difference in reversal activity. The 4-pyridine moiety (**12k**) had dramatic capacity against P-gp, and had the most potential. After reversal evaluation of all target compounds, a clear SAR picture was depicted in **Figure 3**.

Table 3 DOX-resistance reversal activity of target compounds at 1.0 μM concentration in K562/A02 cells [a].

Compound	IC_{50}/DOX (μM)	RF	Compound	IC_{50}/DOX (μM)	RF
12a	11.66 ± 1.04	7.7	**12l**	15.22 ± 2.21	5.9
12b	8.24 ± 0.78	10.9	**12m**	34.54 ± 3.72	2.6
12c	6.15 ± 0.69	14.6	**12n**	6.70 ± 0.31	13.4
12d	11.37 ± 1.31	7.9	**12o**	29.93 ± 3.22	3.0
12e	5.22 ± 0.41	17.2	**12p**	14.97 ± 1.38	6.0
12f	14.25 ± 1.30	6.3	**12q**	27.21 ± 2.74	3.3
12g	5.79 ± 0.41	15.5	**12r**	10.95 ± 1.70	8.2
12h	10.09 ± 1.02	8.9	**12s**	8.89 ± 0.65	10.1
12i	11.97 ± 1.22	7.5	**1**	4.83 ± 0.71	18.6
12j	47.26 ± 4.21	1.9	5.0 μM VRP	21.38 ± 3.71	4.2
12k	2.91 ± 0.12	30.9	Control [b]	89.80 ± 4.52	1.0

[a] The IC_{50} value was determined after exposure to a series of DOX concentration with different target compounds at 1.0 μM using K562/A02 cells; Reversal fold (RF, fold-change in drug sensitivity) = (IC_{50} without inhibitor / (IC_{50} with inhibitor). [b] 0.1% DMSO was added as solvent control. Data were analyzed with GraphPad Prism 5.0 software and presented as mean ± SD for three independent tests.

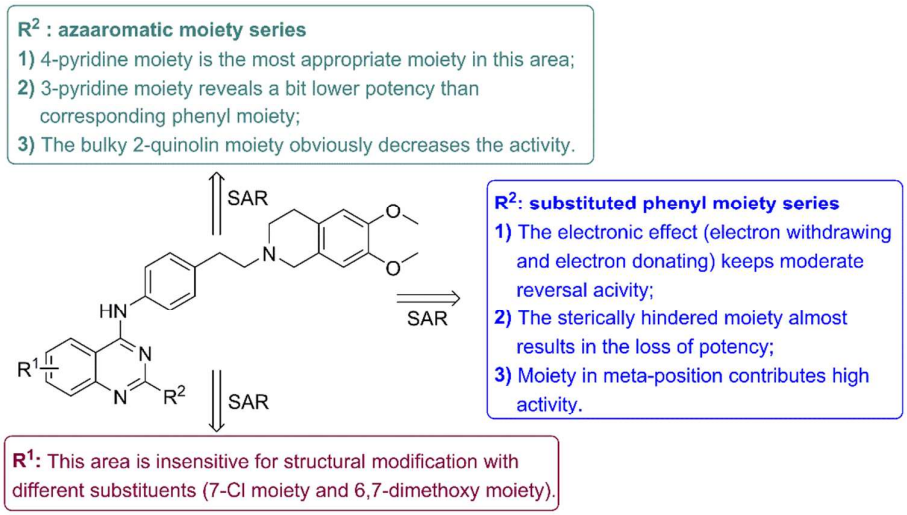

Figure 3. SARs summary of derivatives with quinazoline scaffolds.

Dose–response relationship and selective index (SI) of 12k

Looking forward the quantitative efficacy of the most promising compound **12k** to reverse DOX-resistance, EC_{50} value was determined in K562/A02 cells. EC_{50} refers to the concentration of inhibitor required to reduce the IC_{50} of DOX by half compared with a control without a modulator.[21] Compound **12k** had an EC_{50} of 57.9 ± 3.5 nM for reversing DOX resistance in K562/A02 cells (**Figure 4A**).

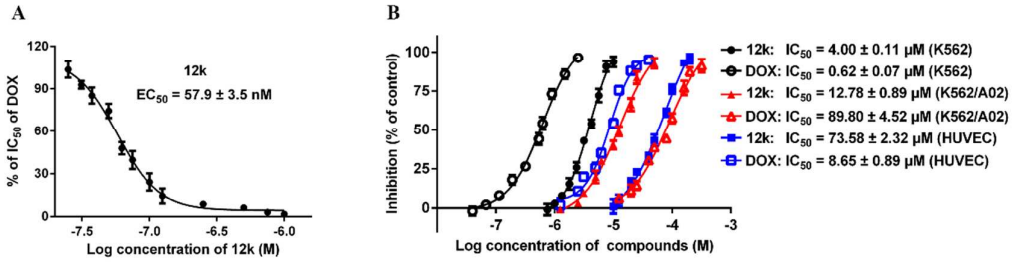

Figure 4. (A) EC_{50} value of **12k** in lowering DOX-resistance in K562/A02 cells. The percent of IC_{50} of DOX was plotted against log concentration of **12k**. The percent of IC_{50} of DOX = [(IC_{50} of DOX at each modulator concentration/ IC_{50} of DOX without modulator) × 100%. EC_{50} is defined as the concentration of modulator that can reduce the % of IC_{50} of DOX by half; **(B)** IC_{50} values of **12k** and DOX in inhibition of K562, K562/A02 and HUVEC cell lines determined by MTT method. The inhibition was plotted against log concentration of **12k** and DOX. Each date point is presented as mean ± SD for three independent tests.

To confirm that the increased cytotoxicity with compound **12k** shown in **Table 3** and **Figure 4A** was due to modulation and not due to the cytotoxicity of **12k** itself, the IC_{50} values were determined for K562 cells and K562/A02 cells. DOX showed a high toxic effect on K562 cells (IC_{50} = 0.62 ± 0.07 μM) and low toxic effect on K562/A02 cells (IC_{50} = 89.80 ± 4.52 μM) (**Figure 4B**), and K562/A02 cells displayed ≈144.8-fold greater resistance than K562 cells. IC_{50} values for compound **12k** to K562 cells and K562/A02 cells were 4.00 μM and 12.78 μM, respectively, which were 75.6- and 241.6-fold of the EC_{50} for compound **12k** in reversing DOX resistance in K562/A02 cells, respectively. Results of the cytotoxicity assay suggested that the enhanced cytotoxicity seen in **Table 3** and **Figure 4A** was a result of the modulatory effect of compound **12k**. The toxicity of **12k** against human umbilical vein endothelial cells (HUVECs) was determined to evaluate its safety: this compound showed no toxic effects towards HUVECs (IC_{50} = 73.58 ± 2.32 μM). The SI (ratio of IC_{50} towards HUVECs to EC_{50} for reversing DOX resistance in K562/A02 cells) for **12k** was very high, up to 1270.8, suggesting that **12k** may be a safe MDR modulator for normal human cells when co-administrated with anticancer agents.

Effect of compound 12k on reversing P-gp-mediated resistance to other anticancer drugs

Resistance to other chemotherapeutic drugs with diverse structures and mechanisms of action is a common phenomenon in MDR. Therefore, whether **12k** can also reverse P-gp-mediated resistance to other P-gp substrates including paclitaxel (PTX), vinblastine (VLB) and daunorubicin (DNR) was evaluated. A non-MDR anticancer drug, cyclophosphamide (CTX), was also selected to verify the reversal potency of compound **12k** on P-gp inhibition. Concentrations

of anticancer drugs were set to 0, 0.313, 0.625, 1.25, 2.5, 5, 10, and 20 μM (**Figure 5**). When co-administered with 1.0 μM **12k** in K562/A02 cells, enhanced toxicity of PTX, VLB and DNR was observed. However, reversal activity was not demonstrated when CTX was co-administered with 1.0 μM **12k** in K562/A02 cells. The results indicated that inhibition of the P-gp function of compound **12k** was responsible for the reversal of resistance.

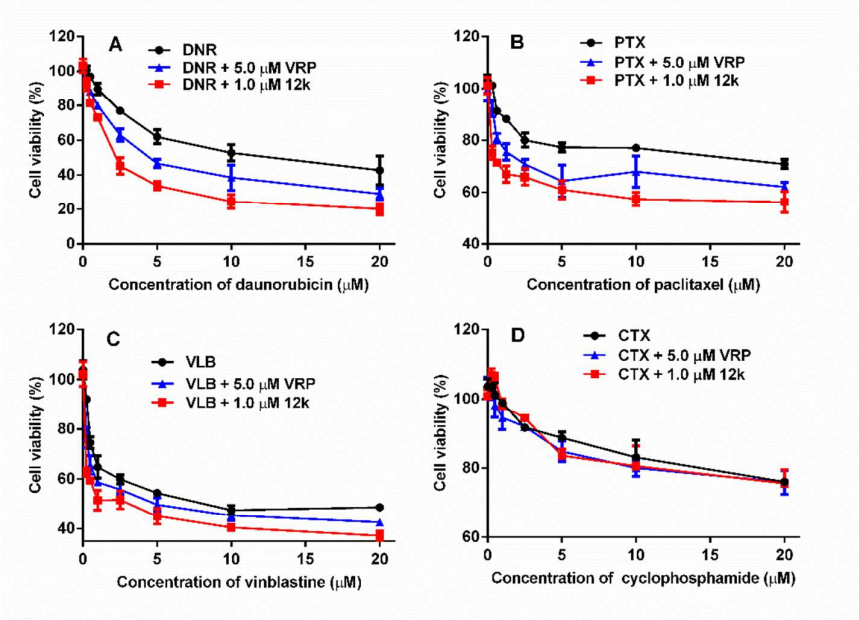

Figure 5. Effect of compound **12k** on reversing other anticancer drugs resistance in K562/A02 cells: A. DNR; B. PTX; C. VLB; D. CTX. DNR, PTX, and VLB are P-gp substrates, whereas CTX is not. Each data point is presented as mean ± SD for three independent tests.

Duration of drug effect

To evaluate the duration of action of compound **12k** as a modulator, K562/A02 cells were incubated with 1.0 μM compound **12k** for 24 h followed by removal of the modulator by washing and incubation for various times in the absence of the reversal agent before DOX addition. VRP (5.0 μM) and phosphate-buffered saline were selected as comparators in this experiment, which was carried out according to a previous report.[9, 22] 5.0 μM VRP and 1.0 μM **12k** displayed strong MDR reversal activity in resistant K562/A02 cells (no-wash group) (**Figure 5**). The MDR-reversing potency of VRP decreased immediately after its removal from the medium. After its removal for 6 h, a MDR-reversing effect was not observed, indicating that the reversal potency

of VRP lasted ≤6 h. In contrast, the MDR reversal effect of compound **12k** was remarkable immediately after its removal. Moreover, **12k** showed effective reversal activity 24 h after its removal from the medium. These results also demonstrated that the MDR-reversing potency of **12k** persisted even after 24-h washout.

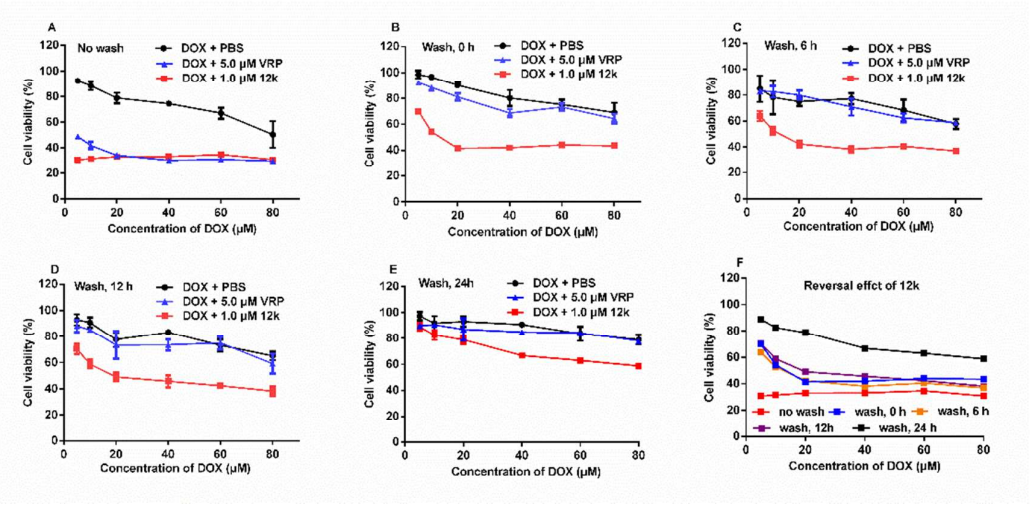

Figure 6. Duration of reversal effect of **12k** and VRP toward DOX in K562/A02 cells after incubation and subsequent washout. Cell viability was determined by MTT assay. Data represents means ± SD of triplicate determinations.

Effect of 12k on DOX accumulation

Due to a defect in accumulation of cytotoxic moieties caused by P-gp, the reversal ability of **12k** correlated to a concomitant increase in DOX accumulation was explored. The auto-fluorescence property of DOX allows an accumulation assay by spectrofluorometry to be carried out. DOX accumulation in K562 cells was about 5.46-fold ($P < 0.001$) higher than that of K562/A02 cells in the absence of a modulator (**Figure 7**), which was due to P-gp-mediated DOX efflux. Even at modulator concentrations down to 0.1 μM, **12k** and **1** enhanced 2.5-h accumulation of DOX into K562/A02 cells significantly ($P < 0.05$), whereas VRP enhanced DOX accumulation only if present at 5.0 μM. These data suggested that **12k** exhibited greater potency in increasing DOX accumulation into K562/A02 cells than VRP, and was also superior to the positive control **1**.

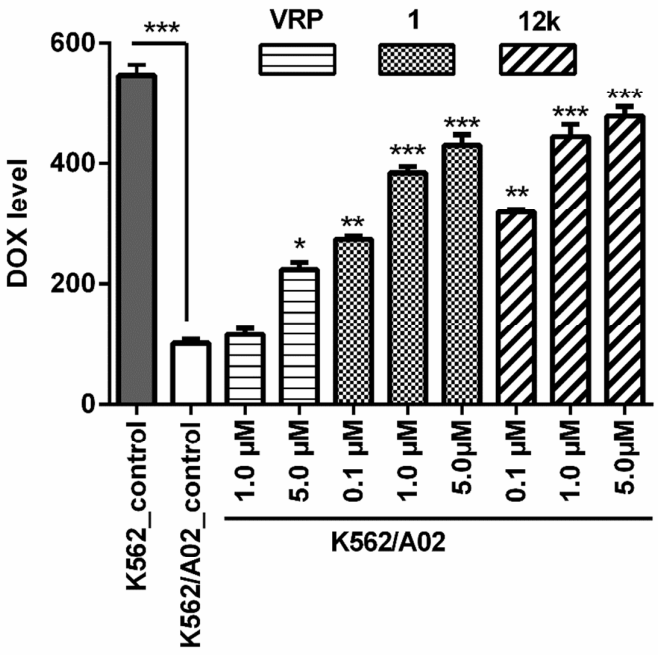

Figure 7. Effect of compound **12k** on intracellular DOX accumulation in K562/A02 cells, with 0.1% DMSO as negative control. The results are presented as the mean ± SD for three independent experiments; (***) $P < 0.001$, (**) $P < 0.01$, (*) $P < 0.05$ relative to the negative control (K562/A02).

Inhibitory effect of 12k on P-gp-mediated Rh123 efflux

It is well known that the potency of MDR modulators on P-gp efflux employs P-gp-dependent efflux of the fluorescent dye Rh123 *via* flow cytometry to evaluate.[23] As demonstrated in **Figure 8**, 1.0 μM **12k** could inhibit Rh123 efflux from K562/A02 cells significantly compared with the control ($P < 0.05$). Moreover, at different time points of 5, 10, 25, 30, 60 and 90 min, intracellular Rh123-associated mean fluorescence intensity (MFI) in 1.0 μM **12k**-treated cells was superior to that in 5.0 μM VRP- and 1.0 μM **1**-treated cells, suggesting that the inhibitory activity of **12k** was more powerful than that of positive controls. These consequences demonstrated **12k** can reverse MDR by inhibiting P-gp-mediated drug efflux.

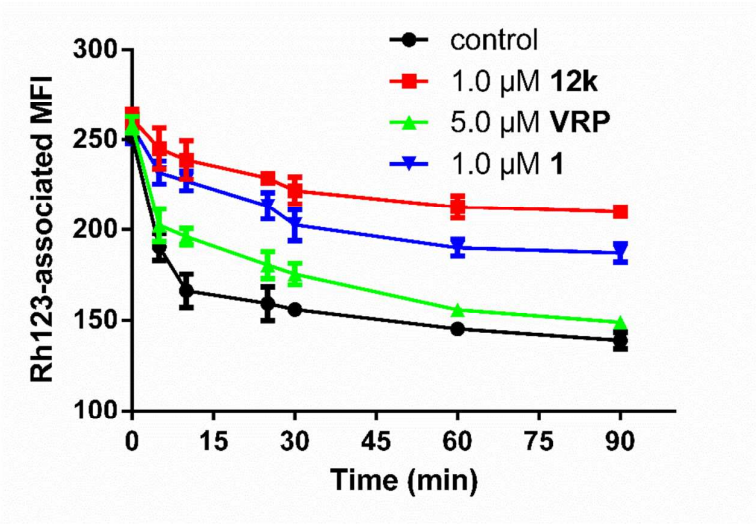

Figure 8. Effect of **12k** on efflux of Rh123 from K562/A02, with 0.1% DMSO as negative control. Each data point is presented as mean ± SD for three independent experiments.

Effect of 12k on P-gp-ATPase activity

In further evaluation, the effect of **12k** on P-gp-ATPase activity was also determined. VRP is not only an inhibitor but a substrate of P-gp, which is proved to be also a stimulator of P-gp-ATPase. P-gp-ATPase activity was strongly increased over the basal level by 2.6-fold by 50.0 μM VRP (**Figure 8**). However, **12k** and **1** exerted inhibition of P-gp-ATPase even at 0.5 μM, which was obviously lower than the basal level (**Figure 9**), suggesting that similar to **1**, compound **12k** could inhibit the activity of P-gp ATPase.

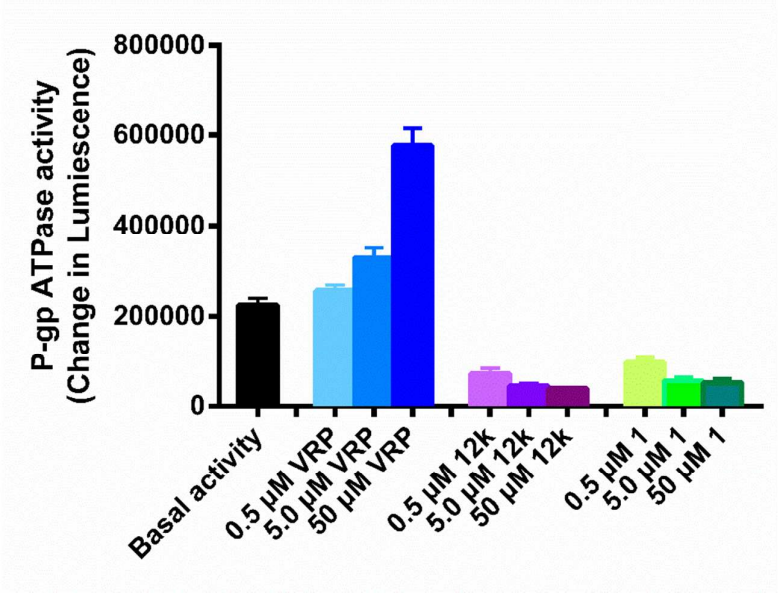

Figure 9. Effect of **12k** on P-gp-ATPase activity. Sodium vanadate-inhibitable ATPase (P-gp ATPase) was studied as described in Experimental Section. P-gp ATPase was measured in the absence (basal activity) or presence of P-gp modulators (VRP, **12k** and **1**). Results are presented as the mean ± SD for three independent experiments.

Effect of 12k on P-gp expression

The presence of P-gp protein was proved by a band with a molecular weight of ≈170 kDa in K562/A02 cell lysates by western blotting. However, it was not present in parental K562 cells, suggesting the absence of P-gp protein (**Figure 10**). Inhibiting the function or lowering expression of P-gp will contribute to the reversal of P-gp-mediated MDR. Therefore, whether the reversal ability of **12k** was due to a decrease in protein expression should be confirmed. Firstly, the cells were incubated with **12k** (0.1, 0.5, or 2.0 μM). Subsequently, the P-gp expression in the cell lysates were determined respectively. There was no evident alteration in P-gp expression in K562/A02 cells (**Figure 10**), indicating that MDR reversal by **12k** was not caused by a decreased protein expression but instead most likely due to direct inhibition of P-gp efflux.

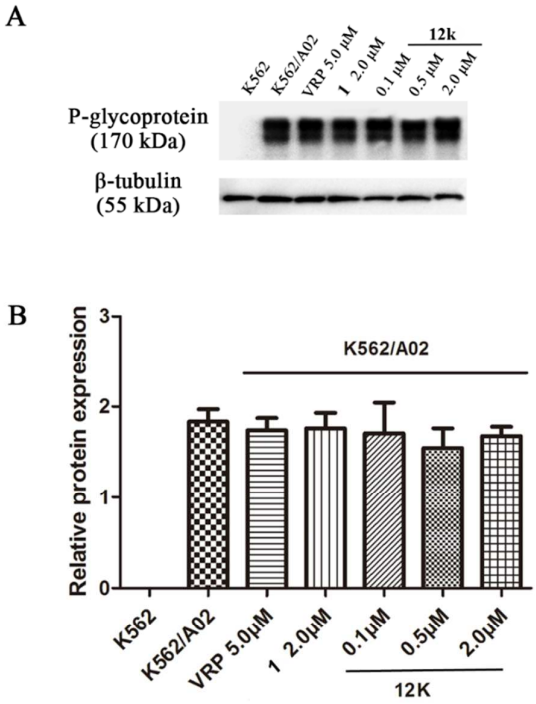

Figure 10. Western blot analysis indicating the expression of ABCB1 after exposure to 0.1, 0.5, or 2.0 μM **12k**. (A) Effect of **12k** at 0.1, 0.5, or 2.0 μM on expression level of ABCB1 in K562/A02 cells for 72 h. (B) Band intensity was analyzed by Quantity One software and protein expression was presented as the ratio of target protein's band intensity to that of β-Tubulin. Representative result is shown here and similar results were obtained in two other independent trials.

Effect of 12k on cytochrome P3A4 (CYP3A4)

There is an impressive overlap between P-gp and CYP3A4 with regard to the characteristics of substrate and tissue distribution. This overlap suggests the presence of several P-gp inhibitors as substrates for CYP3A4 with unexpected pharmacokinetic interactions with chemotherapeutics. To investigate further the characteristics of **12k** as a safe P-gp inhibitor, its *in vitro* inhibitory effect was determined on rat liver CYP3A4 (**Figure 11**). A specific inhibitor of CYP3A4, ketoconazole inhibited CYP3A4 activity in a concentration-dependent manner, whereas **12k** has no effect on CYP3A4 activity even at 40 μM, which was much higher than the EC_{50} *in vitro*. These results demonstrated that **12k** may be a relatively safe P-gp modulator even if co-administered with chemotherapeutics metabolized by CYP3A4.

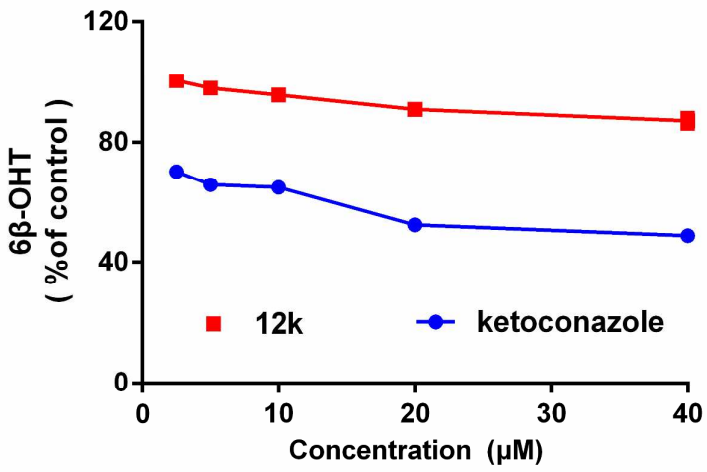

Figure 11. The effect of **12k** and ketoconazole on CYP3A4. Ketoconazole, a specific inhibitor of CYP3A4, was the positive control. 6β-OH testosterone (6β-OHT) is the specific product of

testosterone metabolized by CYP3A4. The data represent the mean ± SD for three independent experiments.

Pharmacokinetics of 12k *in vivo*

To measure the pharmacokinetics of **12k** *in vivo***,** three SD rats in each group were selected to be given **12k** *via* oral or intravenous routes. The standard curve for **12k** was y = 0.0045x + 0.0086 with R^2 = 0.999. Main pharmacokinetic parameters were calculated using Phoenix WinNonlin v6.3 (Certara, Princton, NJ, USA) and are presented in **Table 4**. The peak concentration of **12k** in plasma was 569.6 ± 83.5 ng/mL (1100 ± 161.5 nM), much higher than the EC_{50} value in K562/A02 cells. The half-life ($T_{1/2}$) for **12k** in the intravenous group was 5.9 ± 0.3 h, which was an appropriate duration and much longer than that of the free DOX group ($T_{1/2}$ = 1.6 ± 0.2 h). In addition, **12k** had good bioavailability (≤95.3%).

Table 4 Pharmacokinetic parameters of **12k** (i.v. dose of 5 mg/kg, p.o. of 10 mg/kg) in the plasma of male Sprague–Dawley rats.[a]

Parameter	I.V. (5mg/kg)	P.O. (10mg/kg)
$AUC_{(0-24)}$ (ng·mL^{-1}·h)	1655 ± 151	3131 ± 94
$AUC_{(0-\infty)}$ (ng·mL^{-1}·h)	1754 ± 173	3344 ± 119
$T_{1/2}$ (h)	5.9 ± 0.3	6.2 ± 0.7
C_{max} (ng·mL^{-1})	569.6 ± 83.5	761.2 ± 63.0
CL (ml.min^{-1}kg^{-1})	47.8 ± 2.0	49.9 ± 1.8
F (%)	95.3	

Note: [a] Data are shown as the mean ± SD (n = 3). AUC, area under the curve from zero to 24h or infinity; $T_{1/2}$, elimination half-life; C_{max}, maximum plasma concentration; CL, plasma clearance; F (bioavailability) = $(AUC_{po}/AUC_{iv})*(dose_{iv}/dose_{po})$ *100%

Pharmacokinetics of DOX in rats treated with 12k

In a further study of the effect of **12k** on DOX metabolism, the rat group co-administered VRP and DOX showed an increased plasma concentration of DOX compared with the free-DOX group, suggesting an elevated risk of anthracycline-induced cardiotoxicity. The rat group administered DOX combined with **12k** or **1** had an almost identical metabolism as the group administered free DOX (**Figure 12**). The MDR inhibitor **12k** showed potent MDR reversal activity *in vitro*, but also reached the necessary plasma concentration without drug interactions. Other data also suggested that pharmacokinetic indices ($T_{1/2}$, plasma clearance, mean residence time; data not shown) were not significantly different from that of the free-DOX group *in vivo*. These results suggested that **12k** application could obviate the side-effects closely related to increased plasma concentrations of cytotoxic agents *in vivo*.

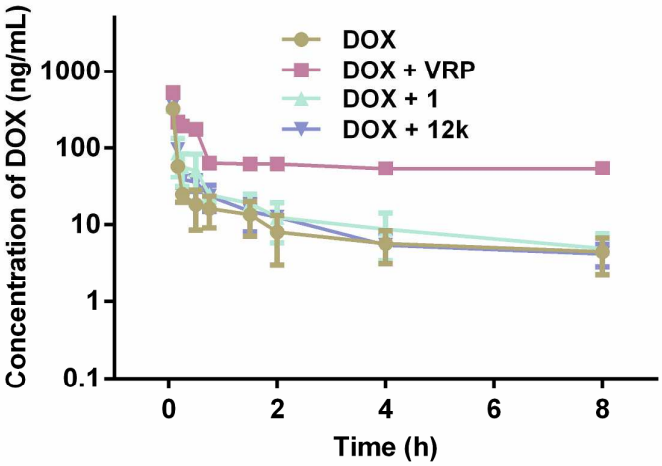

Figure 12. Plasma concentration–time profiles for DOX for the four groups of male Sprague–Dawley rats: group A (free DOX, i.v. dose of 10 mg/kg body mass); group B (DOX + VRP, i.v. dose of 10 mg/kg DOX and 5 mg/kg **VRP**); group C (DOX + **1**, i.v. dose of 10 mg/kg DOX and 5 mg/kg **1**); and group D (DOX + **12k**, i.v. dose of 10 mg/kg DOX and 5 mg/kg **12k**). GraphPad Prism 5.0 software was used for data analysis and the data points are presented as the mean ± SD for three independent tests.

CONCLUSIONS

In this study, a series of novel P-gp-mediated MDR modulators with quinazoline scaffolds were designed and synthesized *via* a convenient procedure. All the structures of the novel compounds

were characterized by NMR, HRMS, and IR spectra. Biological evaluation *in vitro* demonstrated that a few compounds exhibited potent MDR reversal activity. In particular, **12k** exhibited outstanding activity against the P-gp-overexpressing daughter line K562/A02 with a low EC_{50} (57.9 ± 3.5 nM).

This compound showed high survival towards normal cells (IC_{50} = 73.58 ± 2.32 μM), suggesting that the SI of **12k** was very high (1270.8). **12k** also exhibited reversal effects on the other chemotherapeutic drugs that may have different structures and mechanisms of action, such as P-gp substrates (PTX, VLB, DNR) but had no effect on the non-P-gp substrate CTX. The duration of action of **12k** lasted even after 24-h washout.

12k exhibited remarkable potency not in increasing accumulation of DOX into K562/A02 cells, but in inhibiting P-gp-mediated drug efflux of Rh123. Also, **12k** (different from VRP) contributed to inhibition of P-gp-ATPase, which accounted (at least in part) for the mechanism action of MDR reversal. Western-blotting suggested that MDR reversal by **12k** was not due to a decrease in protein expression. More importantly, **12k** did not affect CYP3A4 activity even at high concentrations, and avoided pharmacokinetic interactions *in vitro*. A follow-up in-depth study *in vivo* demonstrated **12k** to have superior pharmacokinetic profiles and not to be susceptible to DOX metabolism. In conclusion, **12k** holds potential for reversing P-gp mediated MDR.

EXPERIMENTAL SECTION

General chemistry

All starting materials, reagents and solvents were obtained from commercial sources and used without further purification unless otherwise indicated. Purifications by column chromatography were carried out over silica gel (200-300 mesh) and monitored by thin layer chromatography (TLC) performed on GF/UV 254 plates and were visualized using UV light at 254 and 365 nm. Melting points were taken on a RY-1 melting-point apparatus and were uncorrected. NMR spectra were recorded in DMSO-d_6 on a Bruker ACF-300Q instrument (300 MHz for ^{1}H, 75 MHz for ^{13}C; Bruker Instruments, Inc., Billerica, MA, USA), chemical shifts are expressed as values (ppm) relative to tetramethylsilane as internal standard, and coupling constants (*J* values) were given in hertz (Hz). Abbreviations are used as follows: s = singlet, d = doublet, t = triplet, q = quartet, m =

multiplet, dd = doublets of doublet, br = broad. Infrared spectras were recorded on a Perkin-Elmer FTIR instrument. ESI-MS datas were recorded with Waters ACQUITY UPLC Systems with Mass (Waters, Milford, MA). High Resolution Mass measurement was performed on Agilent Q-TOF 6520 mass spectrometer with electron spray ionization (ESI) as the ion source. The intermediate **7a-s** [24], **8a-s** [25], **9a-s** [26], **10** [27] and **11** [27] were prepared the following reported procedures (supporting information).

Purities of Target Compounds

The purity of all target compounds was established by UHPLC of Shimadzu LC-30A (SHIMADZU, Japan). The LC was operated as follows: solvent A, 10mM aqueous NaH_2PO_3; solvent B, methanol; column, Shim-pack XR-ODS II (2.2 μm) 100 * 2.0 mm (SHIMADZU, Japan); column temperature, 40 °C; flow rate, 0.4 mL/min; gradient program, 0-5 min: %B = 30-95 gradient, 5-6.5 min: %B = 95, 6.5-7.5 min: %B = 95-30 gradient, 7.5-10 min: %B = 30. UV signals were recorded at 254 nm. The content results of compounds **12a-s** were intelligently calculated with the LabSolution. The purities of all target compounds were >95% for biological evaluation.

General Procedure for the Synthesis of 12a-s

The mixtures of compounds **9a-s** (1 mmol), **11** (1 mmol) and methanesulfonic acid (0.1 mmol) in ethanol (10 ml) were heated to reflux for 4 h. Then the reaction solutions were cooled to room temperature and filtered to give a yellow solid. The resulting solid was added into the 1 N NaOH solution (15 ml) followed by strong stirring for 1 h, and then organic compounds were extracted with DCM (20 ml × 2). Organic layers were washed with water (20 ml), brine (20 ml) respectively and dried over Na_2SO_4. The solvents were filtered and evaporated under reduced pressure to give the crudes. The final compounds **12a-s** was recrystallized from ethanol.

N-(4-(2-(6,7-dimethoxy-3,4-dihydroisoquinolin-2(1H)-yl)ethyl)phenyl)-2-phenylquinazolin-4-amine (12a).

Yellow solid; Yield 52.5%; m.p. 88-90°C ; ^{1}H NMR (300 MHz, DMSO-d_6) δ: 9.82 (s, 1 H, NH), 8.57 (d, J = 8.4 Hz, 1 H, ArH), 8.46-8.43 (m, 2 H, ArH), 7.91-7.85 (m, 4 H, ArH), 7.51-7.49 (m, 3

H, ArH), 7.37-7.34 (m, 3 H, ArH), 6.66, 6.64 (2s, 2 H, ArH), 3.69 (s, 6 H, 2 × OCH_3), 3.57 (s, 2 H, $ArCH_2N$), 2.89-2.72 (m, 8 H, 4 × CH_2); ^{13}C NMR (75 MHz, DMSO-d_6) δ: 157.82, 150.41, 138.32, 137.15, 135.80, 133.11, 130.21, 128.62, 128.35, 128.06, 127.84, 126.65, 125.92, 125.85, 122.94, 122.07, 113.97, 111.73, 109.9, 59.54, 55.42, 55.09, 50.55, 32.47, 28.31; HRMS (ESI) m/z calcd for $[C33H32N4O2+H]^+$ 517.2598, found 517.2588；IR (KBr，cm^{-1}) ν：2932.06, 1560.51, 1515.26, 1416.87, 1358.35, 1255.17, 1227.06, 1227.96, 760.47, 709.58. Purity 96.106 %; t_r 4.128 min.

N-(4-(2-(6,7-dimethoxy-3,4-dihydroisoquinolin-2(1H)-yl)ethyl)phenyl)-2-(2-methoxyphenyl) quinazolin-4-amine (12b).

Yellow solid; Yield 43.7%; m.p. 107-109°C ;^{1}H NMR (300 MHz, DMSO-d_6) δ: 9.73 (s, 1 H, NH), 8.57 (d, J = 8.1 Hz, 1 H, ArH), 7.94-7.79 (m, 4 H, ArH), 7.64-7.59 (m, 2 H, ArH), 7.42 (dd, J = 7.5, 1.7 Hz, 1 H, ArH), 7.24 (d, J = 8.4 Hz, 2 H, AH), 7.14 (d, J = 8.4 Hz, 1 H, ArH), 7.03 (dd, J = 7.5, 7.5 Hz, 1 H, ArH), 6.65, 6.63 (2s, 2 H, ArH), 3.80 (s, 3 H, OCH_3), 3.73 (s, 6 H, 2 × OCH_3), 3.53 (s, 2 H, $ArCH_2N$), 2.80-2.49 (m, 8 H, 4 × CH_2); ^{13}C NMR (75 MHz, DMSO-d_6) δ: 157.06, 146.83, 137.3, 135.3,, 132.8, 130.8, 130.1, 128.4, 127.9, 126.6, 125.8, 122.7, 121.6, 119.9, 113.4, 111.9, 111.7, 109.9, 59.59, 55.49, 55.42, 55.03, 50.55, 32.43, 28.27; HRMS (ESI) m/z calcd for $[C34H34N4O3+H]^+$ 547.2704, found 547.2699；IR (KBr, cm^{-1}) ν: 2832.44, 1245.63, 1601.30, 1516.81, 1463.32, 754.71. Purity 98.180 %; t_r 4.013 min.

N-(4-(2-(6,7-dimethoxy-3,4-dihydroisoquinolin-2(1H)-yl)ethyl)phenyl)-2-(3-methoxyphenyl) quinazolin-4-amine (12c).

Yellow solid; Yield 60.6%; m.p.76-77°C; ^{1}H NMR (300 MHz, DMSO-d_6) δ: 9.83 (s, 1 H, NH), 8.56 (d, J = 7.8 Hz, 1 H, ArH), 8.05-8.01 (m, 2 H, ArH), 7.89-7.84 (m, 4 H, ArH), 7.62-7.59 (m, 1 H, ArH), 7.42-7.31 (m, 3 H, ArH), 7.06-7.04 (m, 1 H, ArH), 6.65, 6.63 (2s, 2 H, ArH), 3.82 (s, 3 H, OCH_3), 3.68 (s, 6 H, 2 × OCH_3), 3.55 (s, 2 H, $ArCH_2N$), 2.85-2.49 (m, 8 H, 4 × CH_2); ^{13}C NMR (75 MHz, DMSO-d_6) δ: 159.3, 158.7, 157.7, 150.4, 147.1, 146.8, 139.8, 137.1, 135.8, 133.0, 129.3, 128.5, 128.0, 126.6, 125.9, 125.8, 122.9, 122.2, 120.2, 116.2, 114.0, 112.6, 111.7, 110.0, 59.5, 55.4, 55.0, 54.9, 50.5, 32.4, 28.2; HRMS (ESI) m/z calcd for $[C34H34N4O3+H]^+$ 547.2704, found 547.2691; IR (KBr, cm^{-1}) ν：3356.93, 2837.76, 1596.32, 1560.54, 1515.47, 1463.21, 1254.07, 1127.30, 762.07, 737.73. Purity 98.480 %; t_r 4.051 min.

N-(4-(2-(6,7-dimethoxy-3,4-dihydroisoquinolin-2(1H)-yl)ethyl)phenyl)-2-(4-methoxyphenyl) quinazolin-4-amine (12d).

Yellow solid; Yield 63.2%; m.p. 125-127°C; ^{1}H NMR (300 MHz, DMSO-d_6) δ: 9.77 (s, 1 H, NH), 8.54 (d, J = 8.4 Hz, 1 H, ArH), 8.41 (d, J = 8.7 Hz, 2 H, ArH), 7.89 (d, J = 8.7 Hz, 2 H, ArH), 7.82 (d, J = 3.8 Hz, 2 H, ArH), 7.57-7.52 (m, 1 H, ArH), 7.32 (d, J = 8.4 Hz, 2 H, ArH), 7.04 (d, J = 8.9 Hz, 2 H, ArH), 6.63, 6.61 (2s, 2 H, ArH), 3.82 (s, 3 H, OCH_3), 3.68 (s, 6 H, 2 × OCH_3), 3.53 (s, 2 H, $ArCH_2N$), 2.85-2.49 (m, 8 H, 4 × CH_2); ^{13}C NMR (75 MHz, DMSO-d_6) δ: 161.10, 158.89, 157.67, 150.54, 147.10, 146.86, 137.20, 129.49, 128.57, 127.85, 126.65, 125.91, 125.30, 122.92, 121.99, 113.68, 111.73, 109.96, 59.52, 55.44, 55.40, 55.19, 55.08, 50.51, 32.48, 28.30; HRMS (ESI) m/z calcd for $[C34H34N4O3+H]^+$ 547.2704, found 547.2703；IR (KBr，cm^{-1}) ν：3309.73, 2825.96, 1606.34, 1572.40, 1515.62, 1452.92, 1228.80, 1170.10, 697.67. Purity 98.419 %; t_r 4.089 min.

N-(4-(2-(6,7-dimethoxy-3,4-dihydroisoquinolin-2(1H)-yl)ethyl)phenyl)-2-(3,4-dimethoxyphenyl) quinazolin-4-amine (12e).

Yellow solid; Yield 56.2%; m.p.158-160°C; ^{1}H NMR (300 MHz, DMSO-d_6) δ: 9.79 (s, 1 H, NH), 8.54 (d, J = 8.4 Hz, 1 H, ArH), 8.06-8.03 (m, 2 H, ArH), 7.79 (d, J = 8.4 Hz, 2 H, ArH), 7.82 (d, J = 3.9 Hz, 2 H, ArH), 7.57-7.53 (m, 1 H, ArH), 7.34 (d, J = 8.4 Hz, 2 H, ArH), 7.07 (d, J = 8.7 Hz, 2 H, ArH), 6.66, 6.64 (2s, 2 H, ArH), 4.04, 4.01 (2s, 6 H, 2 × OCH_3), 3.85-3.83 (2s, 6 H, 2 × OCH_3), 3.56 (s, 2 H, $ArCH_2N$), 2.85-2.49 (m, 8 H, 4 × CH_2); ^{13}C NMR (75 MHz, DMSO-d_6) δ: 158.76, 157.58, 150.74, 148.35, 147.11, 146.87, 137.17, 135.79, 132.98, 130.93, 128.46, 127.86, 126.63, 125.90, 125.31, 122.93, 122.26, 120.92, 113.70, 111.75, 110.97, 109.96, 59.63, 55.50, 55.42, 55.11, 50.55, 32.46, 28.28; HRMS (ESI) m/z calcd for $[C35H36N4O4+H]^+$ 577.2809, found 577.2806; IR (KBr, cm^{-1}) ν: 3380.53, 2837.76, 1593.37, 1570.14, 1516.67, 1463.43, 1235.73, 1177.90, 764.32. Purity 96.705 %; t_r 3.957 min.

N-(4-(2-(6,7-dimethoxy-3,4-dihydroisoquinolin-2(1H)-yl)ethyl)phenyl)-2-(3,4,5-trimethoxyphenyl)quinazolin-4-amine (12f).

Pale yellow solid; Yield 48.4%; m.p. 174-176°C; ^{1}H NMR (300 MHz, DMSO-d_6) δ: 9.86 (s, 1 H, NH), 8.54 (d, J = 8.4 Hz, 1 H, ArH), 7.89-7.81 (m, 6 H, ArH), 7.61-7.56 (m, 1 H, ArH), 7.33 (d, J

= 8.7 Hz, 2 H, ArH), 6.66, 6.64 (2s, 2 H, ArH), 3.87 (s, 6 H, 2 × OCH_3), 3.73, 3.70 (2s, 9 H, 3 × OCH_3), 3.55 (s, 2 H, $ArCH_2N$), 2.87-2.68 (m, 8 H, 4 × CH_2); ^{13}C NMR (75 MHz, DMSO-d_6) δ: 158.37, 157.59, 152.67, 147.11, 146.86, 139.42, 137.06, 135.98, 133.61, 128.38, 127.99, 126.62, 125.89, 125.63, 122.94, 122.52, 113.78, 111.75, 109.97, 104.97, 60.04, 59.68, 55.57, 55.44, 55.08, 50.55, 32.46, 28.27; HRMS (ESI) m/z calcd for $[C36H38N4O5+Na]^+$ 629.2734, found 629.2739; IR (KBr, cm^{-1}) ν：3374.06, 2833.53, 1591.22, 1572.10, 1515,52, 1461.03, 1222.36, 1124.83, 741.71, 766.49. Purity 98.106 %; t_r 3.875min.

2-(benzo[d][1,3]dioxol-5-yl)-N-(4-(2-(6,7-dimethoxy-3,4-dihydroisoquinolin-2(1H)-yl)ethyl)phenyl)quinazolin-4-amine (12g)

Pale yellow solid; Yield 57.1%; m.p.136-139°C; ^{1}H NMR (300 MHz, DMSO-d_6) δ: 9.86 (s, 1 H, NH), 8.57 (d, J = 8.2 Hz, 1 H, ArH), 8.04 (dd, J = 8.2, 1.6 Hz, 1 H, ArH), 7.89-7.86 (m, 3 H, ArH), 7.81-7.93 (m, 2 H, ArH), 7.59-7.53 (m, 1 H, ArH), 7.35 (d, J = 8.4 Hz, 2 H, ArH), 7.03 (d, J = 8.2, 1.6 Hz, 1 H, ArH), 6.71, 6.68 (2s, 2 H, ArH), 6.11 (s, 2 H, OCH_2), 3.82 (s, 2 H, $ArCH_2N$), 3.71, 3.70 (2s, 6 H, 2 × OCH_3), 2.95-2.83 (m, 8 H, 4 × CH_2); ^{13}C NMR (75 MHz, DMSO-d_6) δ: 158.48, 157.67, 150.41, 149.15, 147.48, 147.08, 137.36, 134.74, 133.08, 132.69, 128.93, 128.60, 127.87, 125.50, 125.16, 123.02, 122.56, 122,20, 113.79, 111.65, 109.85, 108.08, 107.60, 101.39, 58.46, 56.39, 55.48, 55.43, 54.06, 50.08, 31.49, 27.19; HRMS (ESI) m/z calcd for $[C34H32N4O4+Na]^+$ 583.2316, found 583.2318; IR (KBr, cm^{-1}) ν: 3327.43, 2902.65, 1593.37, 1558.01, 1517.18, 1443.09，1425.41, 1124.86, 741.80, 774.22. Purity 99.882%; t_r 3.986 min.

N-(4-(2-(6,7-dimethoxy-3,4-dihydroisoquinolin-2(1H)-yl)ethyl)phenyl)-2-(m-tolyl)quinazolin-4-amine (12h).

Pale yellow solid; Yield 53.8%; m.p.138-140°C; ^{1}H NMR (300 MHz, DMSO-d_6) δ: 9.95 (s, 1 H, NH), 8.66 (d, J = 8.4 Hz, 1 H, ArH), 8.30-8.23 (m, 2 H, ArH), 8.01 (d, J = 8.4 Hz, 2 H, ArH), 7.86 (d, J = 3.6 Hz, 2 H, ArH), 7.62-7.57 (m, 1 H, ArH), 7.42-7.37 (m, 3 H, ArH), 7.31 (d, J = 8.4 Hz, 1 H, ArH), 6.78, 6.75 (2s, 2 H, ArH), 4.16 (s, 2 H, $ArCH_2N$), 3.73, 3.72 (2s, 6 H, 2 × OCH_3), 3.12-2.97 (m, 8 H, 4 × CH_2), 2.42 (s, 3 H, CH_3); ^{13}C NMR (75 MHz, DMSO-d_6) δ: 159.06, 157.77, 150.45, 148.01, 147.45, 138.32, 137.91, 137.33, 133.08, 130.84, 128.59, 128.49, 128.26, 127.99, 125.75, 125.11, 124.04, 123.19, 122.21, 114.01, 111.59, 109.75, 56.91, 55.54, 55.49,

52.32, 49.30, 29.96, 25.58, 21.21; HRMS (ESI) m/z calcd for $[C34H34N4O2+H]^+$ 531.2755, found 531.2741; IR (KBr, cm^{-1}) ν: 3287.91, 2934.68, 1618.62, 1559.93, 1520.64, 1463.98, 1449.78, 1123.00, 729.48, 766.31. Purity 97.801%; t_r 4.082 min.

N-(4-(2-(6,7-dimethoxy-3,4-dihydroisoquinolin-2(1H)-yl)ethyl)phenyl)-2-(p-tolyl)quinazolin-4-amine (12i).

Pale yellow solid; Yield 61.1%; m.p.97-100°C; ^{1}H NMR (300 MHz, DMSO-d_6) δ: 9.80 (s, 1 H, NH), 8.57 (d, J = 8.1 Hz, 1 H, ArH), 8.35 (d, J = 8.1 Hz, 2 H, ArH), 7.90 (d, J = 8.3 Hz, 2 H, ArH), 7.84 (d, J = 3.4 Hz, 2 H, ArH), 7.60-7.54 (m, 1 H, ArH), 7.34-7.29 (m, 4 H, ArH), 6.63 (d, J = 6.8 Hz, 2 H, ArH), 3.78, 3.75 (2s, 6 H, 2 × OCH_3), 3.54 (s, 2 H, $ArCH_2N$), 2.84-2.70 (m, 8 H, 4 × CH_2), 1.91 (s, 3 H, CH_3); ^{13}C NMR (75 MHz, DMSO-d_6) δ: 159.11, 157.75, 150.48, 147.12, 146.88, 139.84, 137.19, 135.69, 132.98, 128.94, 128.57, 127.97, 127.88, 126.67, 125.93, 125.54, 122.95, 122.00, 113.93, 111.76, 109.98, 59.48, 55.42, 55.09, 50.49, 32.48, 28.30, 20.95; HRMS (ESI) m/z calcd for $[C34H34N4O2+H]^+$ 531.2755, found 531.2749; IR (KBr, cm^{-1}) ν: 3380.53, 2920.35, 1571.61, 1557.21, 1514.96, 1451.24, 1417.11, 1175.87, 739.87, 763.08. Purity 96.471%; t_r 4.055 min.

2-(4-(tert-butyl)phenyl)-N-(4-(2-(6,7-dimethoxy-3,4-dihydroisoquinolin-2(1H)-yl)ethyl)phenyl)quinazolin-4-amine (12j).

Pale yellow solid; Yield 47.1%，m.p.120-122°C. ^{1}H NMR (300 MHz, DMSO-d_6) δ: 9.79 (s, 1 H, NH), 8.57 (d, J = 8.4 Hz, 1 H, ArH), 8.37 (d, J = 8.4 Hz, 2 H, ArH), 7.91 (d, J = 8.4 Hz, 2 H, ArH), 7.84 (d, J = 3.9 Hz, 2 H, ArH), 7.58-7.51 (m, 3 H, ArH), 7.35 (d, J = 8.4 Hz, 2 H, ArH), 6.65 (d, J = 5.2 Hz, 2 H, ArH), 3.69 (s, 6 H, 2 × OCH_3), 3.57(s, 2 H, $ArCH_2N$), 2.87-2.49 (m, 8 H, 4 × CH_2), 1.33 (s, 9 H, $3CH_3$); ^{13}C NMR (75 MHz, DMSO-d_6) δ: 159.11, 157.73, 152.88, 150.51, 147.13, 146.89, 137.23, 135.73, 135.63, 132.97, 128.57, 128.01, 127.74, 126.65, 125.91, 125.57, 125.11, 122.94, 121.95, 113.94, 111.76, 109.99, 59.53, 55.42, 55.08, 50.54, 34.47, 32.50, 30.99, 28.30; HRMS (ESI) m/z calcd for $[C37H40N4O2+H]^+$ 573.3224, found 573.3223; IR (KBr, cm^{-1}) ν: 3386.43, 2949.85, 1572.74, 1558.01, 1515.61, 1448.99, 1354.70, 1325.23, 1130.76, 763.96, 705.78. Purity 97.291%; t_r 4.039 min.

N-(4-(2-(6,7-dimethoxy-3,4-dihydroisoquinolin-2(1H)-yl)ethyl)phenyl)-2-(pyridin-4-yl)quinazolin-4-amine (12k).

Pale yellow solid; Yield 61.1%; m.p. 180-182°C; ^{1}H NMR (300 MHz, DMSO-d_6) δ: 9.94 (s, 1 H, NH), 8.74 (d, J = 5.5 Hz, 2 H, ArH), 8.64 (d, J = 8.0 Hz, 1 H, ArH), 8.26 (d, J = 5.5 Hz, 2 H, ArH), 7.91 (d, J = 8.4 Hz, 4 H, ArH), 7.91-7.85 (m, 1 H, ArH), 7.36 (d, J = 8.3 Hz, 2 H, ArH), 6.65 ((d, J = 7.0 Hz, 2 H, ArH), 3.70, 3.69 (2s, 6 H, 2 × OCH_3), 3.58 (s, 2 H, $ArCH_2N$), 2.90-2.49 (m, 8 H, 4 × CH_2); ^{13}C NMR (75 MHz, DMSO-d_6) δ: 158.07, 157.25, 150.15, 150.08, 147.11, 146.87, 145.54, 136.82, 136.10, 133.34, 128.65, 128.28, 126.66, 125.91, 123.07, 122.28, 121.72, 114.41, 111.77, 109.98, 59.47, 55.46, 55.43, 55.09, 50.51, 32.49, 28.30; HRMS (ESI) m/z calcd for $[C32H32N5O2+H]^+$ 518.2551, found 518.2547; IR (KBr, cm^{-1}) ν: 3238.94, 1618.77, 1604.08, 1553.35, 1516.65, 1452.10, 1132.92, 771.17, 705.14, 599.42. Purity 99.507%; t_r 3.916 min.

N-(4-(2-(6,7-dimethoxy-3,4-dihydroisoquinolin-2(1H)-yl)ethyl)phenyl)-2-(pyridin-3-yl)quinazolin-4-amine (12l).

Pale yellow solid; Yield 44.8%; m.p. 110-112°C. ^{1}H NMR (300 MHz, DMSO-d_6) δ: 9.92 (s, 1 H, NH), 9.54 (s, 1 H, ArH), 8.68 (d, J = 5.5 Hz, 2 H, ArH), 8.58 (d, J = 8.2 Hz, 1 H, ArH), 7.88-7.84 (m, 4 H, ArH), 7.65-7.61 (m, 1 H, ArH), 7.55-7.50 (m, 1 H, ArH), 7.35 (d, J = 8.2 Hz, 2 H, ArH), 6.64 (d, J = 6.2 Hz, 2 H, ArH), 3.69 (s, 6 H, 2 × OCH_3), 3.55 (s, 2 H, $ArCH_2N$), 2.88-2.50 (m, 8 H, ArH); ^{13}C NMR (75 MHz, DMSO-d_6) δ: 157.89, 157.44, 150.76, 150.53, 150.16, 149.17, 136.90, 135.98, 135.01, 133.65, 133.21, 130.35, 129.79, 128.94, 128.58, 128.03, 126.51, 126.15, 123.48, 123.07, 122.43, 122.31, 114.13, 111.73, 109.95, 59.41, 56.65, 56.06, 55.44, 50.02, 50.45, 38.43, 28.21; HRMS (ESI) m/z calcd for $[C32H31N5O2+H]^+$ 518.2551, found 518.2545; IR (KBr, cm^{-1}) ν: 3333.33, 1601.53, 1570.88, 1559.77, 1516.46, 1450.97, 1125.62, 765.85, 724.87, 704.41. Purity 97.221%; t_r 3.899 min.

N-(4-(2-(6,7-dimethoxy-3,4-dihydroisoquinolin-2(1H)-yl)ethyl)phenyl)-2-(quinolin-2-yl)quinazolin-4-amine(12m).

Pale yellow solid; Yield 43.7%; m.p. 149-151°C; ^{1}H NMR (300 MHz, DMSO-d_6) δ: 9.94 (s, 1 H, NH), 8.67 (d, J = 8.4 Hz, 1 H, ArH), 8.58-8.49 (m, 2 H, ArH), 8.19 (t, J = 8.7 Hz, 3 H, ArH), 8.07-7.82 (m, 4 H, ArH), 7.72-7.65 (m, 2 H, ArH), 7.37 (d, J = 8.4 Hz, 2 H, ArH), 6.67 (d, J = 5.2

Hz, 2 H, ArH), 3.69-3.65 (m, 8 H, 2 × OCH_3, $ArCH_2N$), 2.89-2.77 (m, 8 H, 4 × CH_2); ^{13}C NMR (75 MHz, DMSO-d_6) δ: 158.38, 158.14, 154.84, 149.17, 148.29, 147.65, 147.35, 138.11, 136.81, 133.60, 132.33, 130.01, 129.67, 128.73, 128.08, 127.89, 127.61, 127.48, 126.89, 123.52, 123.38, 122.34, 120.72, 120.03, 114.27, 111.52, 109.66, 55.95, 55.57, 55.52, 51.26, 48.85, 29.05, 24.53; HRMS (ESI) m/z calcd for $[C36H33N5O2+H]^+$ 568.2707, found 568.2703; IR (KBr, cm^{-1}) ν: 3345.13, 2932.15, 1625.09, 1554.08, 1519.24, 1430.03, 1242.20, 1121.92, 776.29, 680.98. Purity 95.851%; t_r 3.934 min.

N-(4-(2-(6,7-dimethoxy-3,4-dihydroisoquinolin-2(1H)-yl)ethyl)phenyl)-2-(3-nitrophenyl)quinazolin-4-amine (12n).

Pale yellow solid; Yield 59.5%，m.p.140-142°C. ^{1}H NMR (300 MHz, DMSO-d_6) δ: 10.01 (s, 1 H, NH), 9.16 (d, J = 1.4 Hz, 1 H, ArH), 8.76 (dd, J = 7.8, 1.0 Hz, 1 H, ArH), 8.61 (d, J = 8.1 Hz, 1 H, ArH), 8.31-8.27 (m, 1 H, ArH), 7.91-7.83 (m, 4 H, ArH), 7.75 (t, J = 8.0 Hz, 1 H, ArH), 7.65-7.60 (m, 1 H, ArH), 7.36 (d, J = 8.4 Hz, 2 H, ArH), 6.69 (d, J = 5.2p Hz, 2 H, ArH), 3.82 (s, 2 H, $ArCH_2N$), 3.70 (s, 6 H, 2 × OCH_3), 2.96-2.83 (m, 8 H, 4 × CH_2); ^{13}C NMR (75 MHz, DMSO-d_6) δ: 157.94, 156.80, 150.09, 148.01, 147.45, 147.09, 139.96, 137.10, 135.05, 133.62, 133.28, 129.92, 128.55, 128.11, 126.36, 125.14, 124.53, 123.13, 122.45, 122.24, 114.18, 111.67, 109.86, 58.50, 55.44, 54.04, 50.06, 31.54, 27.24; HRMS (ESI) m/z calcd for $[C33H31N5O4+H]^+$ 562.2449, found 562.2447; IR (KBr, cm^{-1}) ν: 3321.53, 1618.38, 1561.53, 1529.34, 1514.99, 1465.83, 1345.84, 1118.46, 734.62, 714.80, 527.67. Purity 97.189%; t_r 3.972 min.

N-(4-(2-(6,7-dimethoxy-3,4-dihydroisoquinolin-2(1H)-yl)ethyl)phenyl)-2-(4-nitrophenyl)quinazolin-4-amine (12o).

Pale yellow solid; Yield 55.4%; m.p.181-183°C. ^{1}H NMR (300 MHz, DMSO-d_6) δ: 9.95 (s, 1 H, NH), 8.65-8.59 (m, 3 H, ArH), 8.33 (d, J = 7.8 Hz, 2 H, ArH), 7.92-7.85 (m, 4 H, ArH), 7.70-7.64 (m, 1 H, ArH), 7.37 (d, J = 8.4 Hz, 2 H, ArH), 6.66, 6.64 (2s, 2 H, ArH), 3.69 (s, 6 H, 2 × OCH_3), 3.58 (s, 2 H, $ArCH_2N$), 2.88-2.73 (m, 8 H, 4 × CH_2); ^{13}C NMR (75 MHz, DMSO-d_6) δ: 157.91, 157.10, 150.09, 148.32, 147.12, 146.88, 144.32, 136.82, 136.02, 133.30, 128.78, 128.63, 128.25, 126.62, 125.90, 123.48, 123.02, 122.23, 114.11, 111.74, 109.97, 59.48, 55.45, 55.40, 55.08, 50.52, 32.53, 28.30; HRMS (ESI) m/z calcd for $[C33H31N5O4+H]^+$ 562.2449, found 562.2442; IR (KBr,

cm^{-1}) ν: 3427.73, 1598.89, 1565.44, 1517.05, 1408.10, 1340.47, 1129.12, 847.85, 760.95, 716.46. Purity 97.685%; t_r 3.991 min.

2-(4-chlorophenyl)-N-(4-(2-(6,7-dimethoxy-3,4-dihydroisoquinolin-2(1H)-yl)ethyl)phenyl)quinazolin-4-amine (12p).

Pale yellow solid; Yield 41.2%，m.p. 113-115°C; ^{1}H NMR (300 MHz, DMSO-d_6) δ: 9.86 (s, 1 H, NH), 8.57 (d, J = 8.4 Hz, 1 H, ArH), 8.44-8.40 (m, 2 H, ArH), 7.86-7.83 (m, 4 H, ArH), 7.64-7.54 (m, 3 H, ArH), 7.34 (d, J = 8.4 Hz, 2 H, ArH), 6.64 (d, J = 6.3 Hz, 2 H, ArH), 3.69 (s, 6 H, 2 × OCH_3), 3.56 (s, 2 H, $ArCH_2N$), 2.88-2.71 (m, 8 H, 4 × CH_2); ^{13}C NMR (75 MHz, DMSO-d_6) δ: 158.02, 157.84, 150.27, 147.11, 146.86, 137.88, 137.23, 137.02, 135.80, 135.01, 133.08, 130.38, 129.81, 129.52, 128.95, 128.57, 128.34, 128.01, 126.58, 125.88, 123.03, 122.14, 121.10, 113.99, 111.69, 59.43, 56.04, 55.43, 55.38, 55.05, 50.44, 32.45, 28.26; HRMS (ESI) m/z calcd for [C33H31ClN4O2+H]$^+$ 551.2208, found 551.2213; IR (KBr, cm^{-1}) ν: 3356.93, 2914.45, 1599.26, 1571.54, 1557.29, 1516.07, 1255.77, 1166.55, 762.99. Purity 97.037%; t_r 3.945 min.

N-(4-(2-(6,7-dimethoxy-3,4-dihydroisoquinolin-2(1H)-yl)ethyl)phenyl)-2-(4-fluorophenyl)quinazolin-4-amine (12q).

Pale yellow solid; Yield 61.1%，m.p.125-127°C. ^{1}H NMR (300 MHz, DMSO-d_6) δ: 9.91 (s, 1 H, NH), 8.57 (d, J = 8.3 Hz, 1 H, ArH), 8.49-8.44 (m, 2 H, ArH), 7.87-7.82 (m, 4 H, ArH), 7.62-7.57 (m, 1 H, ArH), 7.44-7.28 (m, 4 H, ArH), 6.66, 6.64 (2s, 2 H, ArH), 3.69 (s, 6 H, 2 × OCH_3), 3.59 (s, 2 H, $ArCH_2N$), 2.89-2.50 (m, 8 H, 4 × CH_2); ^{13}C NMR (75 MHz, DMSO-d_6) δ: 165.23, 161.95, 158.09, 157.81, 150.34, 147.13, 146.86, 138.22, 137.10, 135.68, 134.84, 133.39, 132.97, 130.03, 128.92, 128.53, 127.93, 126.48, 125.67, 123.05, 122.14, 121.07, 115.23, 114.94, 113.90, 111.66, 109.89, 105.40, 59.69, 59.36, 56.50, 55.95, 55.40, 55.34, 54.98, 50.35, 32.39, 28.20; HRMS (ESI) m/z calcd for [C33H31FN4O2+H]$^+$ 535.2504, found 535.2496; IR (KBr, cm^{-1}) ν: 3268.44, 2825.96, 1572.93, 1560.94, 1516.70, 1454.88, 1254.06, 1144.73, 748.55, 760.48. Purity 97.018%; t_r 3.938 min.

7-chloro-N-(4-(2-(6,7-dimethoxy-3,4-dihydroisoquinolin-2(1H)-yl)ethyl)phenyl)-2-phenylquinazolin-4-amine (12r).

Pale yellow solid; Yield 61.1%; m.p.105-107°C. ^{1}H NMR (300 MHz, DMSO-d_6) δ: 9.93 (s, 1 H, NH), 8.60 (d, J = 9.0 Hz, 1 H, ArH), 8.46-8.43 (m, 2 H, ArH), 7.89-7.86 (m, 3 H, ArH), 7.62 (dd, J = 8.8, 1.9 Hz, 1 H, ArH), 7.51-7.49 (m, 4 H, ArH), 7.34 (d, J = 8.3 Hz, 2 H, ArH), 6.63 (d, J = 7.7 Hz, 2 H, ArH), 3.70 (s, 6 H, 2 × OCH_3), 3.54 (s, 2 H, $ArCH_2N$), 2.87-2.70 (m, 8 H, 4 × CH_2); ^{13}C NMR (75 MHz, DMSO-d_6) δ: 160.22, 157.67, 151.48, 147.10, 146.86, 137.97, 137.67, 136.83, 136.00, 130.47, 128.59, 128.33, 128.01, 126.69, 126.62, 125.97, 125.89, 125.22, 122.14, 112.66, 111.72, 109.94, 59.44, 55.43, 55.40, 55.07, 50.46, 32.46, 28.29; HRMS (ESI) m/z calcd for $[C33H31ClN4O2+H]^+$ 55.2208, found 551.2192; IR (KBr, cm^{-1}) ν: 2932.15, 1612.18, 1556.36, 1514.65, 1450.47, 1226.96, 1127.38, 768.53, 706.75. Purity 98.670%; t_r 3.850min.

N-(4-(2-(6,7-dimethoxy-3,4-dihydroisoquinolin-2(1H)-yl)ethyl)phenyl)-6,7-dimethoxy-2-phenyl quinazolin-4-amine (12s)

Pale yellow solid; Yield 52.3%; m.p. 120-122°C; ^{1}H NMR (300 MHz, DMSO-d_6) δ: 9.50 (s, 1 H, NH), 8.44 (dd, J = 8.0, 2.0 Hz, 2 H, ArH), 7.88-7.83 (m, 3 H, ArH), 7.51-7.44 (m, 3 H, ArH), 7.33 (d, J = 8.4 Hz, 2 H, ArH), 7.27 (s, 1 H, ArH), 6.62 (d, J = 7.9 Hz, 2 H, ArH), 3.97, 3.95 (2s, 6 H, 2 × OCH_3), 3.70, 3.69 (2s, 6 H, 2 × OCH_3), 3.54 (s, 2 H, $ArCH_2N$), 2.87-2.69 (m, 8 H, 4 × CH_2); ^{13}C NMR (75 MHz, DMSO-d_6) δ: 157.50, 156.47, 154.29, 148.73, 147.56, 147.10, 146.86, 138.73, 137.47, 135.30, 129.66, 128.53, 128.23, 127.50, 126.66, 125.92, 121.95, 111.71, 109.94, 107.64, 107.50, 102.09, 59.51, 56.18, 55.70, 55.43, 55.39, 55.08, 54.84, 50.47, 32.48, 28.30; HRMS (ESI) m/z calcd for $[C35H36N4O4+H]^+$ 577.2809, found 577.2811; IR (KBr, cm^{-1}) ν: 3374.63, 2825.96, 1602.21, 1560.96, 1514.62, 1460.77, 1225.42, 1163.17, 780.11, 702.90. Purity 98.227%; t_r 3.786 min.

Material and Methods

Materials and animals

3-(4,5-dimethylthiazol-2-yl)-2,5-diphenyltetrazolium bromide (MTT), doxorubicin (DOX), daunorubicin (DNR), vinblastine (VLB), paclitaxel (PTX), cyclophosphamide (CTX), verapamil (VRP), rhodamine 123 (Rh123) and dimethyl sulfoxide (DMSO) were purchased from Sigma-Aldrich (St. Louis, MO, USA). WK-X-34 was synthesized by our laboratory before. Monoclonal antibody against ABCB1 (ab170904) was obtained from Abcam plc, USA.

α/β-Tubulin (#2148) and anti-rabbit IgG (#7074) were provided by Cell Signaling Technology, Inc, USA. Pgp-Glo™ assay systems were purchased from Promega Corporation, USA. RPMI 1640s were from Life Technologies, Inc. All common chemicals were in analytical or higher grade. Sprague−Dawley (SD) rats (male, 200−250 g) were purchased from the Comparative Medical Center of Yangzhou University (Jiangsu, China). All animal experimental protocols adhered to the Guide for the Care and Use of Laboratory Animals published by the National Institutes of Health (NIH Publication 85-23, revised 1986), and our experiments have been approved by the institutional committee of China Pharmaceutical University.

Cell lines and cell culture

Human leukemia sensitive cell line K562 and its doxorubicin-selected P-gp overexpressing daughter cell line K562/A02 were kindly provided by Professor Bao-An Chen (Department of Hematology, The Affiliated Zhong-Da Hospital, Southeast University (Nanjing, China). Human umbilical vein endothelial cell line (HUVEC) was purchased from KeyGEN BioTECH (Nanjing, China). The cell lines were grown in RPMI-1640 medium supplemented with 10% heat-inactivated fetal bovine serum (FBS) in a humidified incubator at 37°C with 5% CO_2. To confirm drug resistance characteristics, 1 mg/ml ADM was added to K562/A02 cultures and maintained in drug-free medium for 2 weeks before usage. The cells in exponential growth can be used for experiments.

Methods

Cytotoxicity assay

Cell viability was determined by MTT method with a minor modification.[28-31] K562 and K562/A02 cells during logarithmic growth phase were seeded in 96-well micro-titer plates at 1×10^4 cells per well. P-gp inhibitors were prepared as 5 mM DMSO stocks. In the MTT assay for MDR reversal experiments, cells were incubated in the presence of anticancer agents (DOX, DNR, VLB, PTX or CTX) with or without P-gp inhibitors for 48h. MTT dye (10 μl of 2.5 mg/ml in PBS) was added to each well 4 hours priors to experiment termination in a 37 °C incubator containing 5% CO_2. The plates were then centrifuged at 1500 RPM for 15 min and the supernatant was discarded without disturbing the formazan crystals and cells in the wells, while the MTT formazan crystals

were dissolved in 150 μL of DMSO, and the plates agitated on a plate shaker for 5 min. The optical density (OD) was read on a microplate reader (Thermo, USA) with a wavelength of 490 nm. The IC_{50} values of the compounds for cytotoxicity were calculated by GraphPad Prism 5.0 software (GraphPad software, San Diego, CA, USA) from the dose–response curves.

Duration of the MDR reversal

The experiment was performed as the modified reported procedures previously.[32] Briefly, 1×10^4 K562/A02 cells per well were incubated for 24 h with 1.0 μM of compound **12k**, 5.0 μM VRP or PBS before being washed 0 or 3 times with growth medium. Then, the cells were incubated for 0, 6, 12, or 24 h before the addition of varying concentrations of DOX or vehicle. The incubation was lasted for 48 h prior to the MTT analysis.

Accumulation of doxorubicin

The reported procedures with minor modification was employed for the detection of accumulation of DOX.[21, 33] In brief, 4×10^5 cells of K562 and K562/A02 were incubated with 20.0 μM DOX and different concentrations of compound **12k,** VRP or **1** for 150 min at 37 °C, with 0.1% DMSO as a negative control. After incubation, the cells were washed with cold PBS and lysed with lysis buffer (0.75 M HCl, 0.2% Triton-X100 in isopropanol). The fluorescence level of DOX in the lysate was measured by fluorescence spectrophotometer (RF-5301 PC, SHIMADZU) using an excitation and an emission wavelength pair of 460 and 587 nm.

Efflux of Rh123

On the basis of previous report,[34, 35] K562/A02 cells were incubated with medium containing 5 μM Rh123 at 37°C for 90 min, washed for three times with Rh123-free medium, and then incubated in the presence or absence of different concentrations of **12k,** VRP and **1** at 37°C for 5, 10, 25, 30, 60, and 90 min, respectively. The mean fluorescence intensity (MFI) of retained Rh123 in per 10000 cells was measured by flow cytometry. Graphs were plotted of cell-associated MFI against time.

P-gp ATPase assay

P-gp-Glo™ assay system (Promega, USA) was used to determine the influence of compound **12k** on P-gp ATPase relying on the ATP dependence of the light-generating reaction of firefly luciferase .[36, 37] Firstly, approximately 25 μg of human P-gp membrane fraction was incubated with (1) 100 μM sodium vanadate and 0.5% DMSO, (2) 0.5% DMSO, (3) 0.5 μM, 5.0 μM and 50.0 μM of VRP VRP, (4) 0.5 μM, 5.0 μM and 50.0 μM of **12k** and (5) 0.5 μM, 5.0 μM and 50.0 μM of **1**, respectively. Secondly, addition of 5.0 mM MgATP initiated the reaction and then the plate was incubated at 37 °C for 1 h. Then after incubation, a luminescence signal of luciferase generated by addition of ATP detection reagent was determined as the remaining unmetabolized ATP. Finally, the plate was incubated for further 20 min at room temperature for signal stabilization and then the luminescence signal was measured with GloMax-20/20 luminometer (Promega). The dropped luminescence intensities of samples compared to that treated with sodium vanadate were defines as ATPase activity.

Western blot analysis

The western blot procedure was conducted based on the methods reported previously.[38, 39] Cells were incubated with the predetermined concentrations of **12k**, **1** or VRP respectively for 72 h prior to the protein quantification to confirm whether **12k** can affect the expression of P-gp or not. Cellular proteins from K562 and K562/A02 cells were extracted in the RIPA lysis buffer containing PMSF. Protein concentration was measured by BCA method following the procedures of the kit. Cell lysate (100 μg) was resolved on gradient SDS-PAGE gel and then transferred to PVDF membranes, which were then blocked in blocking solution (5% skim milk) in TBST buffer (10 mM Tris–HCl, pH 8.0, 150 mM NaCl, and 0.1% Tween 20) to block nonspecific binding for 1 h at room temperature. Membranes were subsequently incubated overnight at 4 °C with the primary antibodies (anti-P-gp antibody or β-Tubulin antibody). Thereafter, the membranes were washed three times with TBST buffer and incubated at room temperature for 2 h with HRP-conjugated secondary antibody. After washing for another three times, the detection of enzyme-linked chemiluminescence was performed based on the ECL kit. β-Tublin was used to confirm equal loading in each lane in the samples prepared from cell lysates. Band intensity was

analyzed by Quantity One software and protein expression was presented as the ratio of target protein's band intensity to that of β-Tubulin, the house-keeping gene, in the same blot.

CYP3A4 assays

Differential centrifugation separated Rat liver microsomes and the Bradford was employed to determine the protein concentration.[40] As modified previous description, the activity of CYP3A4 was evaluated with testosterone (substrate of CYP3A4) and HPLC analysis.[41, 42] Based on the content of 6β-OH testosterone (6β-OHT), the specific product of testosterone metabolized by CYP3A4, the effect of the target compound on CYP3A4 could be determined.[43] The octyldecylsilyl (C18) reverse-phase HPLC column (5 mm, 150 mm, 4.6 mm) was used for analysis. The gradient HPLC method was the following: column temperature, 35 °C; flow rate, 1.0 mL/min; mobile phase A, water; mobile phase B, acetonitrile; gradient program, 0-7.5 min: % B = 35, 7.5-14.0 min: % B = 35-48 gradient, 14.0-19.0 min: % B = 48-35 gradient. UV absorbance was detected at 254 nm. The LC-Solution was employed for intelligent calculation of the areas of peaks. The liver microsomes were incubated with testosterone (50 mM) in the absence or presence of **12k** and positive control ketoconazole (a specific inhibitor of CYP3A4) at different concentrations of 2.5 μM, 5.0 μM, 10.0 μM, 20.0 μM and 40.0 μM.

Pharmacokinetics assessment

The pharmacokinetics of **12k** were assessed in the rats as our previous studies.[11, 44] Various concentrations of **12k** (1000.0, 300.0, 150.0, 80.0, 30.0, 10.0, 5ng·mL^{-1}) were prepared to set up a standard curve, with **6** (5.0 μg·mL^{-1}) as the internal standard. The standard curve was plotted with concentration of **12k** on the X axis and the ratio of **12k** area under the peak (AUC) to that of the internal standard on the Y axis. Firstly, the drugs were dissolved in the mixture solution of Tween-80-ethanol- saline (5:10:85, v/v) to treat the rats by oral administration or intravenous injection (p.o. dose of 10 mg/kg, i.v. of 5 mg/kg). Secondly, at 5, 15, 30, and 45 min, and 1, 2, 4, 6, 8, 12, and 24 h after administration, we collected blood from the retro-orbital plexus into heparin-coated tubes. Thirdly, centrifuge at 900g for 10 min to separate the plasma of the blood samples to store at -78 °C until analysis. 50 μL IS solution and 150 μL methanol were respectively

added into 50 μL aliquot of plasma sample ,well mixed, and centrifuged at 9000 rpm for 10 min. Finally, 5.0 μL of the supernatant was analyzed on Waters ACQUITY UPLC Systems with Mass (LC-MS/MS, Waters, Milford, MA). The mobile phase was composed of methanol- ammonium formate (5 mM)-formic acid (55:45:0.2, v/v/v), and was delivered isocratically at a flow rate of 0.25 mL/min and determined at wavelength of 254 nm.

Influence of 12k on DOX metabolism *in vivo*

It is important to confirm whether the necessary plasma concentration of **12k** to reverse MDR *in vitro* affected the metabolism of DOX *in vivo*. Based on the method described above, a standard curve was plotted with DNR as the internal standard (0.5 $\mu g \cdot mL^{-1}$). Experimental animals were randomly divided into 4 groups: group A (free DOX, i.v. dose of 10 mg/kg body mass); group B (DOX + VRP, i.v. dose of 10 mg/kg DOX and 5 mg/kg VRP); group C (DOX + **1**, i.v. dose of 10 mg/kg DOX and 5 mg/kg **1**); and group D (DOX + **12k**, i.v. dose of 10 mg/kg DOX and 5 mg/kg **12k**). At 5, 10, 15, 30, 45 and 90 min, and 2, 4, and 8 h after administration, orbital blood samples were collected respectively. The next steps and analysis were the same as described in pharmacokinetics assessment.

ASSOCIATED CONTENT

Supporting Information

Synthetic procedures and characterization of intermediates **7a-s**, **8a-s**, **9a-s**, **10** and **11**; ^{1}H and ^{13}C NMR spectra, ESI-HRMS spectra and HPLC chromatograms of compounds **12a-s**.

Molecular formula strings and some data (CSV)

AUTHOR INFORMATION

Authors

[#]Qianqian Qiu and [#]Baomin Liu contributed equally to the first author.

Corresponding Authors

*Wenlong Huang, E-mail: ydhuangwenlong@126.com. Phone: +86-25-83271302. Fax: +86-25-83271480.

*Hai Qian, E-mail: qianhai24@163.com. Phone: +86-25-83271302. Fax: (+86-25-83271480.

Notes

The authors declare no competing financial interest.

ACKNOWLEDGMENTS

This work was supported by National Science Foundation of China (NO. 81173088 and NO. 81273376) and the National Science and Technology Major Project of the Ministry of Science and Technology of China (No. 2009ZX09102-033).

ABBREVIATIONS

P-gp, P-glycoprotein; MDR, multidrug resistance; ABC, ATP binding cassette; TKI, tyrosine kinase inhibitor; HPLC, high performance liquid chromatography; DOX, doxorubicin; RF, reversal fold; SI, selective index; VRP, verapamil; PTX, paclitaxel; VLB, vinblastine; DNR, daunorubicin; CTX, cyclophosphamide; phosphate buffered saline; Rh123, rhodamine 123; MFI, mean fluorescence intensity; DMSO, dimethyl sulfoxide; TFA, trifluoroacetic acid; TLC, thin layer chromatography; DCM, dichloromethane; CL, plasma clearance; MRT, mean residence time; MTT, 3-(4,5-dimethylthiazol-2-yl)-2,5-diphenyltetrazolium bromide; HUVEC, human umbilical vein endothelial cell; FBS, fetal bovine serum; UHPLC, Ultra High Performance Liquid Chromatography.

REFERENCES

(1) Gottesman, M. M. Mechanisms of cancer drug resistance. *Annu. Rev. Med.* **2002,** *53*, 615-627. (2) Fojo, A. T.; Ueda, K.; Slamon, D. J.; Poplack, D. G.; Gottesman, M. M.; Pastan, I.

Expression of a multidrug-resistance gene in human tumors and tissues. *Proc. Natl. Acad. Sci. U. S. A.* **1987,** *84*, 265-269.

(3) Quintieri, L.; Fantin, M.; Vizier, C. Identification of molecular determinants of tumor sensitivity and resistance to anticancer drugs. *Adv. Exp. Med. Biol.* **2007,** *593*, 95-104.

(4) Dean, M.; Allikmets, R. Complete characterization of the human abc gene family. *J. Bioenerg.* **2002,** *33*, 475-479.

(5) Colabufo, N. A.; Berardi, F.; Cantore, M.; Contino, M.; Inglese, C.; Niso, M.; Perrone, R. Perspectives of p-glycoprotein modulating agents in oncology and neurodegenerative diseases: Pharmaceutical, biological, and diagnostic potentials. *J. Med. Chem.* **2009,** *53*, 1883-1897.

(6) Sarkadi, B.; Homolya, L.; Szakács, G.; Váradi, A. Human multidrug resistance abcb and abcg transporters: Participation in a chemoimmunity defense system. *Physiol. Rev.* **2006,** *86*, 1179-1236.

(7) Aller, S. G. Structure of p-glycoprotein reveals a molecular basis for poly-specific drug binding. *Science* **2009,** *323*, 1718-1722.

(8) Binkhathlan, Z.; Lavasanifar, A. P-glycoprotein inhibition as a therapeutic approach for overcoming multidrug resistance in cancer: Current status and future perspectives. *Curr. Cancer Drug Targets* **2013,** *13*, 326-346.

(9) Mistry, P.; Stewart, A. J.; Dangerfield, W.; Okiji, S.; Liddle, C.; Bootle, D.; Plumb, J. A.; Templeton, D.; Charlton, P. In vitro and in vivo reversal of p-glycoprotein-mediated multidrug resistance by a novel potent modulator, xr9576. *Cancer Res.* **2001,** *61*, 749-758.

(10) Kim, T. E.; Lee, H.; Lim, K. S.; Lee, S.; Yoon, S. H.; Park, K. M.; Han, H.; Shin, S. G.; Jang, I. J.; Yu, K. S. Effects of hm30181, a p‐glycoprotein inhibitor, on the pharmacokinetics and pharmacodynamics of loperamide in healthy volunteers. *Br. J. Clin. Pharmacol.* **2014,** *78*, 556-564.

(11) Jekerle, V.; Klinkhammer, W.; Scollard, D. A.; Breitbach, K.; Reilly, R. M.; Piquette‐Miller, M.; Wiese, M. In vitro and in vivo evaluation of wk‐x‐34, a novel inhibitor of p‐glycoprotein and bcrp, using radio imaging techniques. *Int. J. Cancer* **2006,** *119*, 414-422.

(12) Müller, H.; Pajeva, I. K.; Globisch, C.; Wiese, M. Functional assay and structure–activity relationships of new third-generation p-glycoprotein inhibitors. *Bioorg. Med. Chem.* **2008,** *16*, 2448-2462.

(13)Nesi, G.; Colabufo, N. A.; Contino, M.; Perrone, M. G.; Digiacomo, M.; Perrone, R.; Lapucci, A.; Macchia, M.; Rapposelli, S. Sar study on arylmethyloxyphenyl scaffold: Looking for a p-gp nanomolar affinity. *Eur. J. Med. Chem.* **2014,** *76*, 558-566.

(14) Palmeira, A.; Sousa, E.; Vasconcelos, M. H.; Pinto, M. M. Three decades of p-gp inhibitors: Skimming through several generations and scaffolds. *Curr. Med. Chem.* **2012,** *19*, 1946-2025.

(15) Ling, Z.; Ma, S. Efflux pump inhibitors: A strategy to combat p-glycoprotein and the nora multidrug resistance pump. *ChemMedChem* **2010,** *5*, 811–822.

(16) Sharom, F. J. Complex interplay between the p-glycoprotein multidrug efflux pump and the membrane: Its role in modulating protein function. *Front. Oncol.* **2014,** *4*, 41-41.

(17) Shi, Z.; Peng, X.-X.; Kim, I.-W.; Shukla, S.; Si, Q.-S.; Robey, R. W.; Bates, S. E.; Shen, T.; Ashby, C. R.; Fu, L.-W. Erlotinib (tarceva, osi-774) antagonizes atp-binding cassette subfamily b member 1 and atp-binding cassette subfamily g member 2–mediated drug resistance. *Cancer Res.* **2007,** *67*, 11012-11020.

(18) Leggas, M.; Panetta, J. C.; Zhuang, Y.; Schuetz, J. D.; Johnston, B.; Bai, F.; Sorrentino, B.; Zhou, S.; Houghton, P. J.; Stewart, C. F. Gefitinib modulates the function of multiple atp-binding cassette transporters in vivo. *Cancer Res.* **2006,** *66*, 4802-4807.

(19) Dai, C.-l.; Tiwari, A. K.; Wu, C.-P.; Su, X.-d.; Wang, S.-R.; Liu, D.-g.; Ashby, C. R.; Huang, Y.; Robey, R. W.; Liang, Y.-j. Lapatinib (tykerb, gw572016) reverses multidrug resistance in cancer cells by inhibiting the activity of atp-binding cassette subfamily b member 1 and g member 2. *Cancer Res.* **2008,** *68*, 7905-7914.

(20) Krapf, M. K.; Wiese, M. Synthesis and biological evaluation of 4-anilino-quinazolines and -quinolines as inhibitors of breast cancer resistance protein (abcg2). *J. Med. Chem.* **2016,** *59*, 5449-5461.

(21) Chan, K. F.; Wong, I. L. K.; Kan, J. W. Y.; Yan, C. S. W.; Chow, L. M. C.; Chan, T. H. Amine linked flavonoid dimers as modulators for p-glycoprotein-based multidrug resistance:

Structure–activity relationship and mechanism of modulation. *J. Med. Chem.* **2012,** *55*, 1999-2014.

(22) Liu, B.; Qiu, Q.; Zhao, T.; Jiao, L.; Li, Y.; Huang, W.; Qian, H. 6, 7 - dimethoxy - 2 - {2 - [4 - (1h - 1, 2, 3 - triazol - 1 - yl) phenyl] ethyl} - 1, 2, 3, 4 - tetrahydroisoquinolines as superior reversal agents for p - glycoprotein - mediated multidrug resistance. *ChemMedChem* **2015,** *10*, 336-344.

(23) Ludescher, C.; Thaler, J.; Drach, D.; Drach, J.; Spitaler, M.; Gattringer, C.; Huber, H.; Hofmann, J. Detection of activity of p - glycoprotein in human tumour samples using rhodamine 123. *Br. J. Haematol.* **1992,** *82*, 161-168.

(24) Rose, U. 2-aryl-substituted 4 h -3,1-benzoxazin-4-ones as novel active substances for the cardiovascular system. *J. Heterocycl. Chem.* **1991,** *28*, 2005–2012.

(25) Lee, E. S.; Son, J. K.; Na, Y. H.; Jahng, Y. Synthesis and biological properties of selected 2-aryl-4(3h)-quinazolinones. *Heterocycl. Commun.* **2004,** *10*, 325-330.

(26) Alafeefy, A. M.; Kadi, A. A.; Al-Deeb, O. A.; El-Tahir, K. E. H.; Al-Jaber, N. A. Synthesis, analgesic and anti-inflammatory evaluation of some novel quinazoline derivatives. *Eur. J. Med. Chem.* **2010,** *45*, 4947-4952.

(27) Klinkhammer, W.; Müller, H.; Globisch, C.; Pajeva, I. K.; Wiese, M. Synthesis and biological evaluation of a small molecule library of 3rd generation multidrug resistance modulators. *Biorg. Med. Chem.* **2009,** *17*, 2524-2535.

(28) Fu, L. W.; Zhang, Y. M.; Liang, Y. J.; Yang, X. P.; Pan, Q. C. The multidrug resistance of tumor cells was reversed by tetrandrine in vitro and in xenografts derived from human breast adenocarcinoma mcf-7/adr cells. *Eur. J. Cancer* **2002,** *38*, 418-426.

(29) Jabbar, S.; Twentyman, P.; Watson, J. The mtt assay underestimates the growth inhibitory effects of interferons. *Br. J. Cancer* **1989,** *60*, 523.

(30) Wang, N.-N.; Zhao, L.-J.; Wu, L.-N.; He, M.-F.; Qu, J.-W.; Zhao, Y.-B.; Zhao, W.-Z.; Li, J.-S.; Wang, J.-H. Mechanistic analysis of taxol-induced multidrug resistance in an ovarian cancer cell line. *Asian Pac. J. Cancer Prev.* **2013,** *14*, 4983-4988.

(31) Sargent, J.; Taylor, C. Appraisal of the mtt assay as a rapid test of chemosensitivity in acute myeloid leukaemia. *Br. J. Cancer* **1989,** *60*, 206.

(32) Liu, B.; Qiu, Q.; Zhao, T.; Lei, J.; Hou, J.; Li, Y.; Qian, H.; Huang, W. Discovery of novel p-glycoprotein-mediated multidrug resistance inhibitors bearing triazole core via click chemistry. *Chem. Biol. Drug Des.* **2014,** *84*, 182–191.

(33) Wong, I.; Chan, K.; Tsang, K.; Lam, C.; Zhao, Y.; Chan, T.; Chow, L. Modulation of multidrug resistance protein 1 (mrp1/abcc1)-mediated multidrug resistance by bivalent apigenin homodimers and their derivatives. *J. Med. Chem.* **2009,** *52*, 5311-5322.

(34) Ji, B. S.; He, L. Cjy, an isoflavone, reverses p-glycoprotein-mediated multidrug-resistance in doxorubicin-resistant human myelogenous leukaemia (k562/dox) cells. *J. Pharm. Pharmacol.* **2007,** *59*, 1011–1015.

(35) Twentyman, P. R.; Rhodes, T.; Rayner, S. A comparison of rhodamine 123 accumulation and efflux in cells with p-glycoprotein-mediated and mrp-associated multidrug resistance phenotypes. *Eur. J. Cancer* **1994,** *30A*, 1360-1369.

(36) Chan, K. F.; Zhao, Y.; Burkett, B. A.; Wong, I. L.; Chow, L. M.; Chan, T. H. Flavonoid dimers as bivalent modulators for p-glycoprotein-based multidrug resistance: Synthetic apigenin homodimers linked with defined-length poly(ethylene glycol) spacers increase drug retention and enhance chemosensitivity in resistant cancer cells. *J. Med. Chem.* **2006,** *49*, 6742-6759.

(37) Ambudkar, S. V. [37] drug-stimulatable atpase activity in crude membranes of human mdr1 -transfected mammalian cells. *Methods Enzymol.* **1998,** *292*, 504-514.

(38) Wang, Y. J.; Kathawala, R. J.; Zhang, Y. K.; Patel, A.; Kumar, P.; Shukla, S.; Fung, K. L.; Ambudkar, S. V.; Talele, T. T.; Chen, Z. S. Motesanib (amg706), a potent multikinase inhibitor, antagonizes multidrug resistance by inhibiting the efflux activity of the abcb1. *Biochem. Pharmacol.* **2014,** *90*, 367-378.

(39) Mudududdla, R.; Guru, S. K.; Wani, A.; Sharma, S.; Joshi, P.; Vishwakarma, R. A.; Kumar, A.; Bhushan, S.; Bharate, S. B. 3-(benzo [d][1, 3] dioxol-5-ylamino)-n-(4-fluorophenyl) thiophene-2-carboxamide overcomes cancer chemoresistance via inhibition of angiogenesis and p-glycoprotein efflux pump activity. *Org. Biomol. Chem.* **2015,** *13*, 4296-4309.

(40) Bradford; Marion M. A rapid sensitive method for the quantization of microgram quantities of protein utilizing the principle of protein-dye binding. *Anal. Biochem*. **1976**, *72*, 248-254.

(41) Kuramochi, M.; Fukuhara, H.; Nobukuni, T.; Kanbe, T.; Maruyama, T.; Ghosh, H. P.; Pletcher, M.; Isomura, M.; Onizuka, M.; Kitamura, T. Tslc1 is a tumor-suppressor gene in human non-small-cell lung cancer. *Nat. Genet.* **2001,** *27*, 427-430.

(42) Dai, C. L.; Xiong, H. Y.; Tang, L. F.; Zhang, X.; Liang, Y. J.; Zeng, M. S.; Chen, L. M.; Wang, X. H.; Fu, L. W. Tetrandrine achieved plasma concentrations capable of reversing mdr in vitro and had no apparent effect on doxorubicin pharmacokinetics in mice. *Cancer Chemother. Pharmacol.* **2007,** *60*, 741-750.

(43) Dai, D.; Tang, J.; Rose, R.; Hodgson, E.; Bienstock, R. J.; Mohrenweiser, H. W.; Goldstein, J. A. Identification of variants of cyp3a4 and characterization of their abilities to metabolize testosterone and chlorpyrifos. *J. Pharmacol. Exp. Ther.* **2001,** *299*, 825-831.

(44) Zhao, T.; Song, Y.; Liu, B.; Qiu, Q.; Jiao, L.; Li, Y.; Huang, W.; Qian, H. Reversal of p-glycoprotein-medicated multidrug resistance by lbm-a5 in vitro and a study of its pharmacokinetics in vivo. *Can. J. Physiol. Pharmacol.* **2014,** *93*, 33-38.

Table of Contents graphic

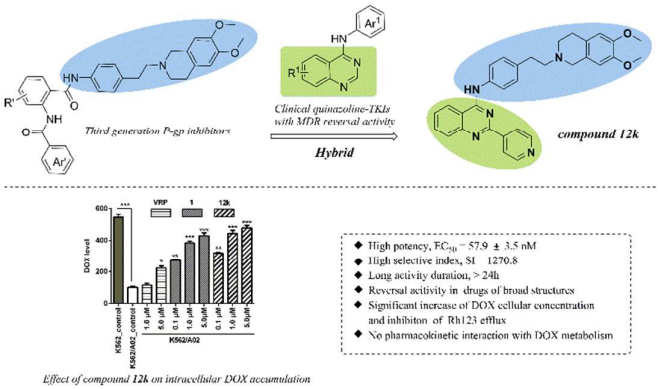

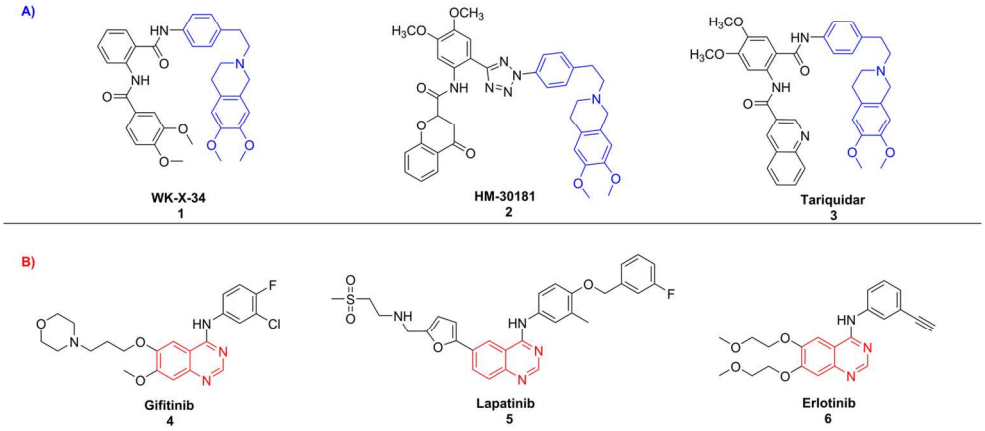

136x69mm (300 x 300 DPI)

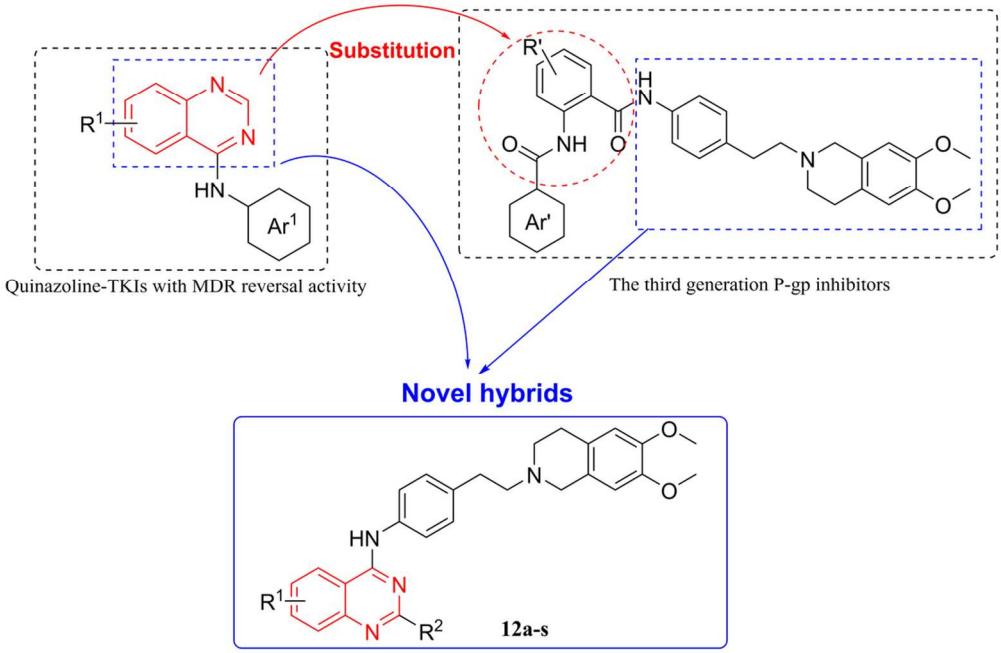

106x69mm (300 x 300 DPI)

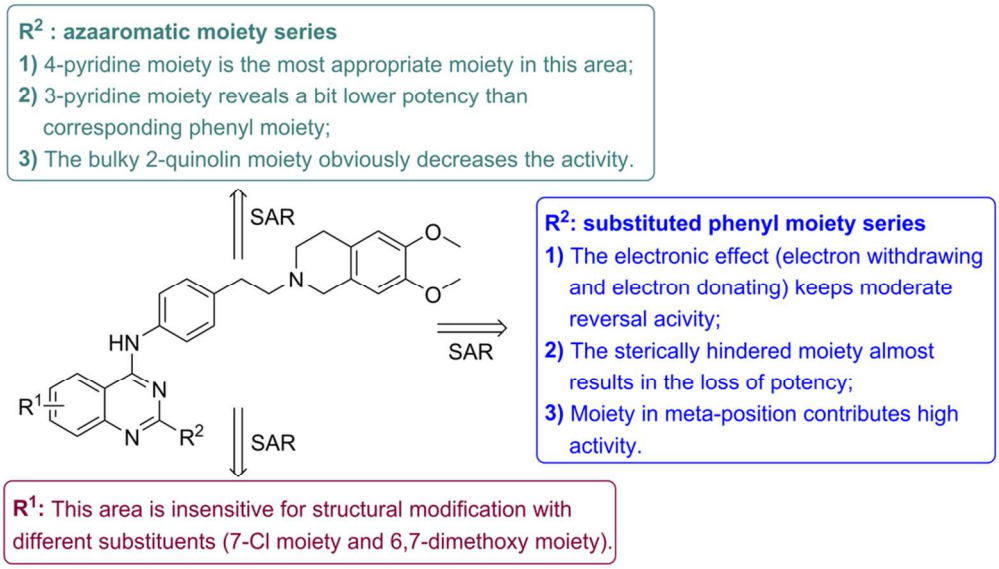

91x51mm (300 x 300 DPI)

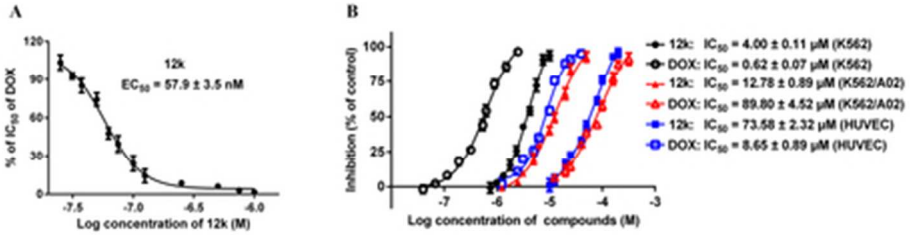

39x10mm (300 x 300 DPI)

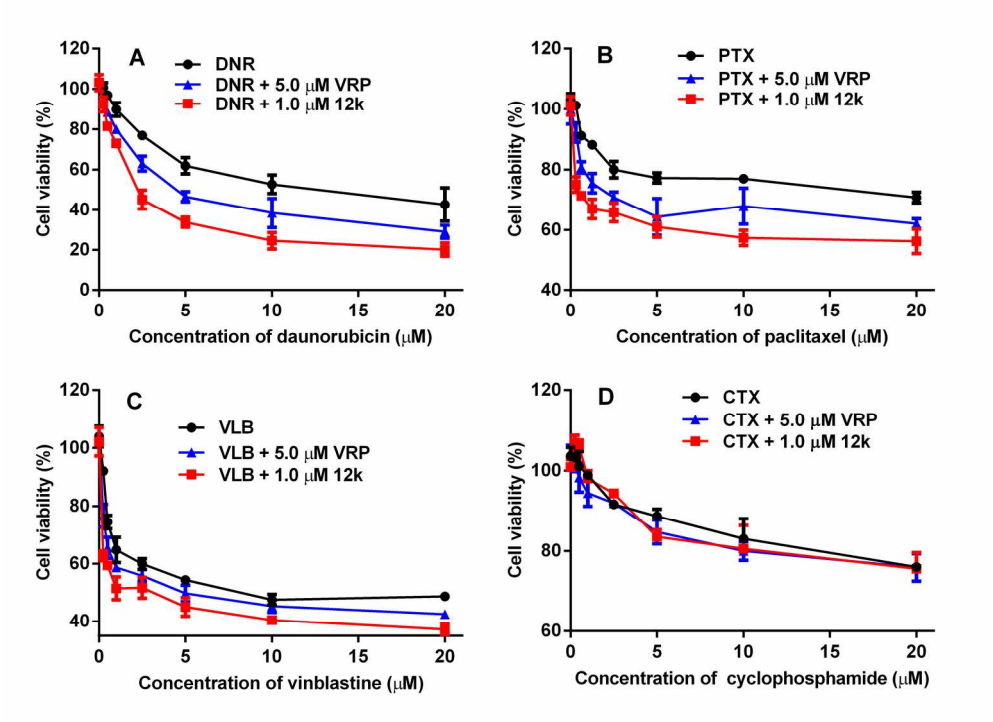

182x132mm (300 x 300 DPI)

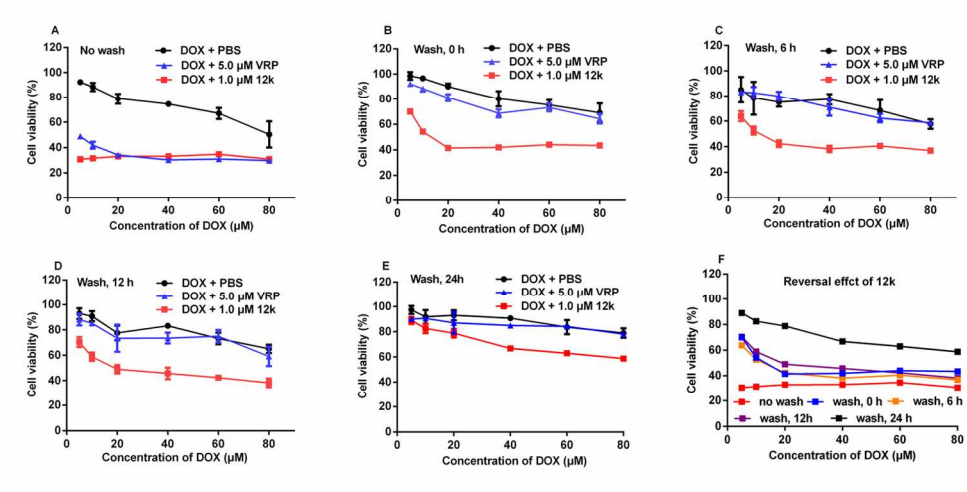

135x66mm (300 x 300 DPI)

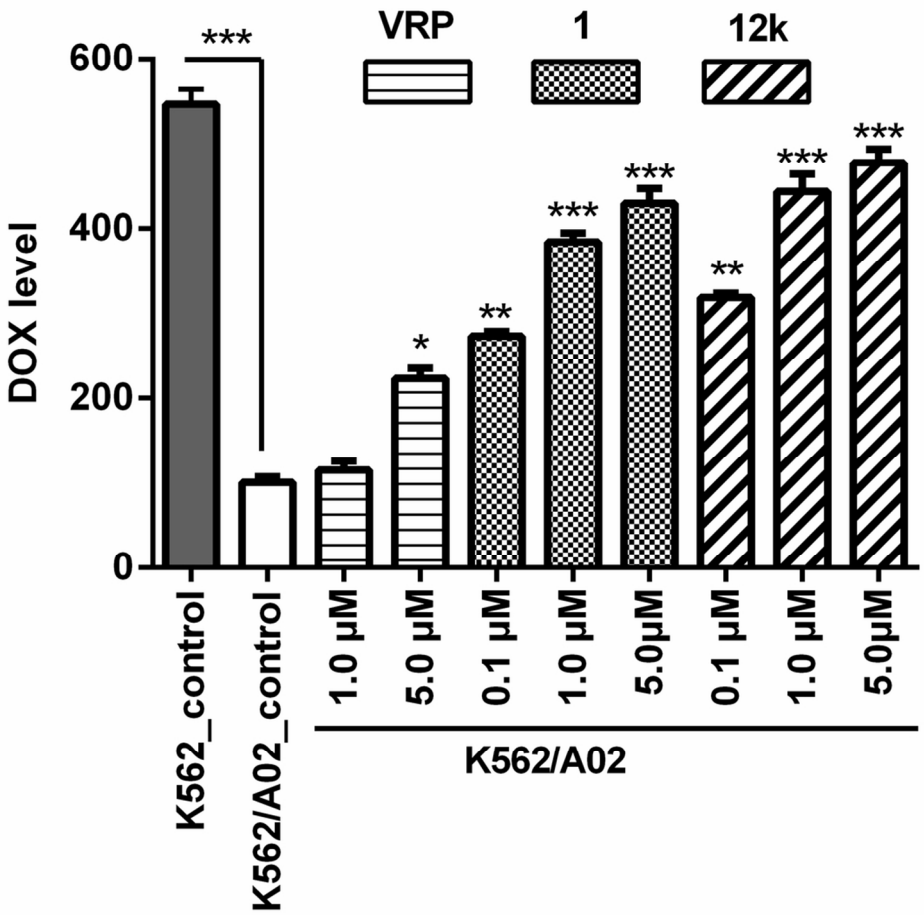

97x95mm (300 x 300 DPI)

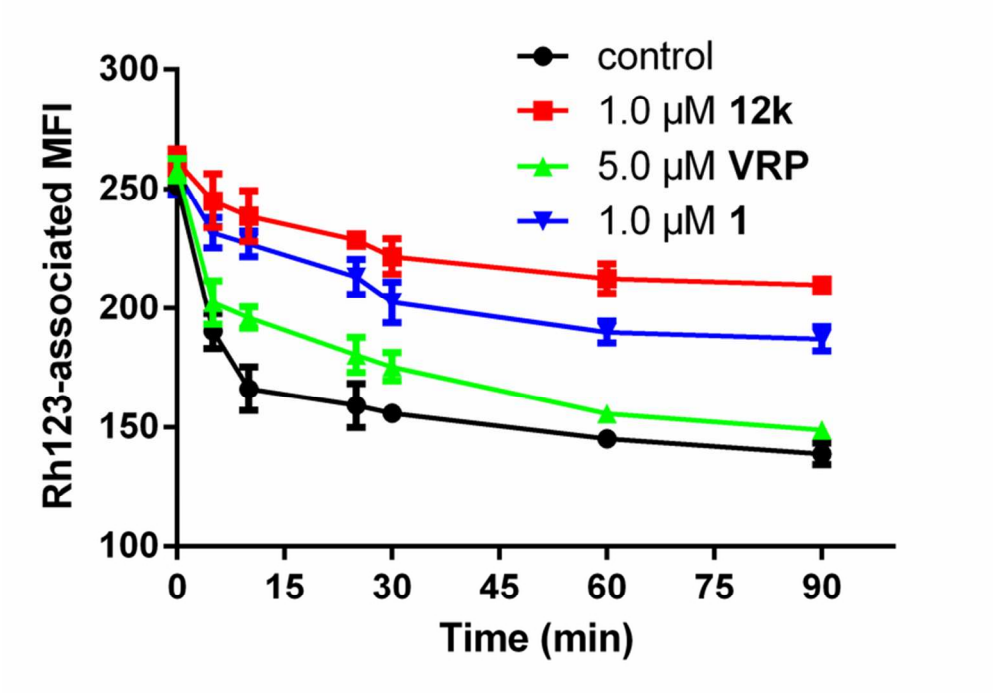

73x51mm (300 x 300 DPI)

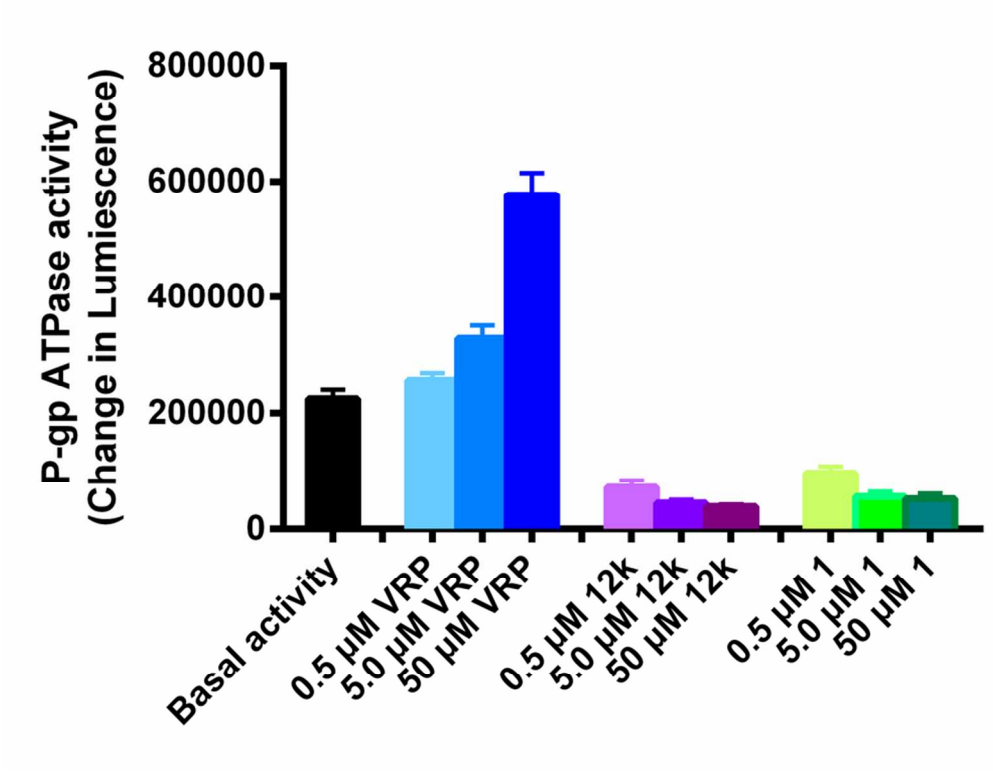

84x64mm (300 x 300 DPI)

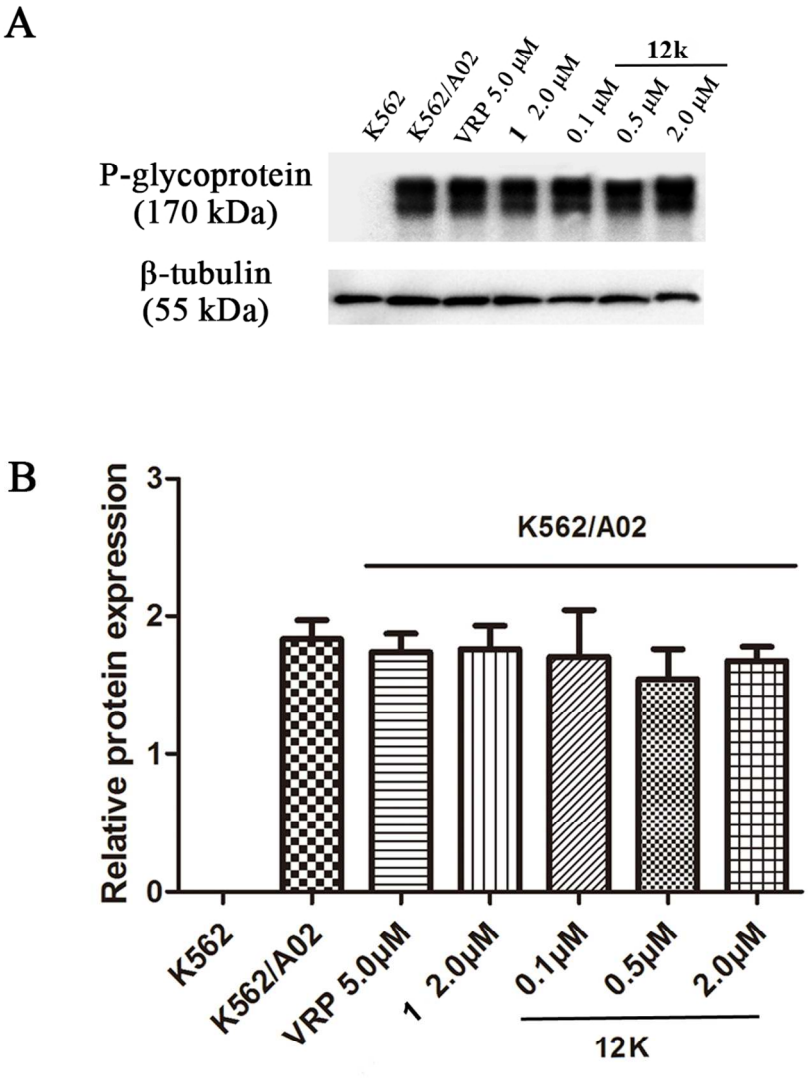

101x126mm (299 x 299 DPI)

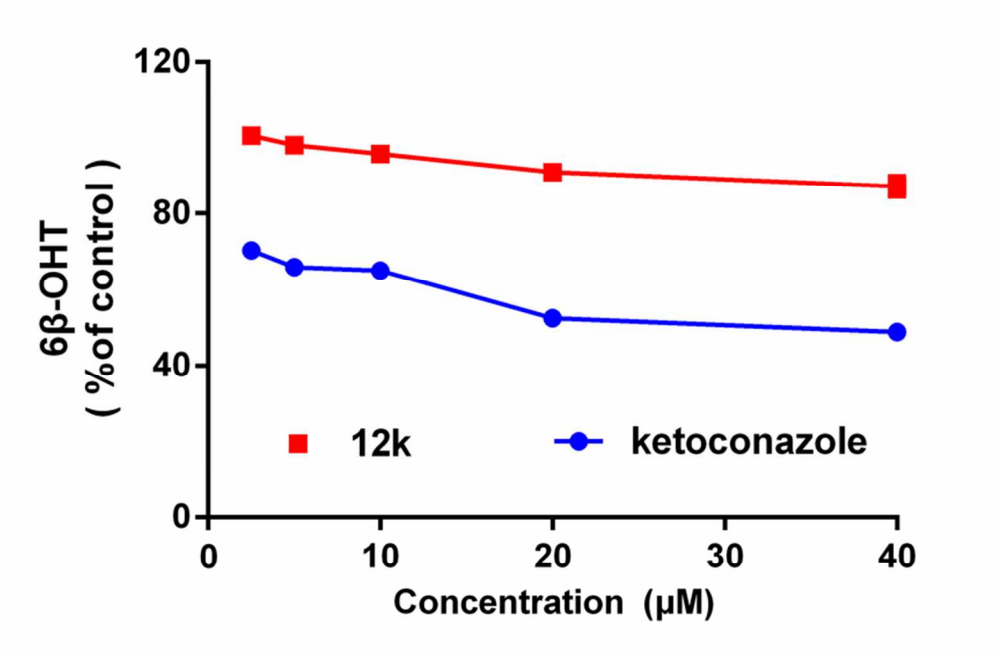

73x48mm (300 x 300 DPI)

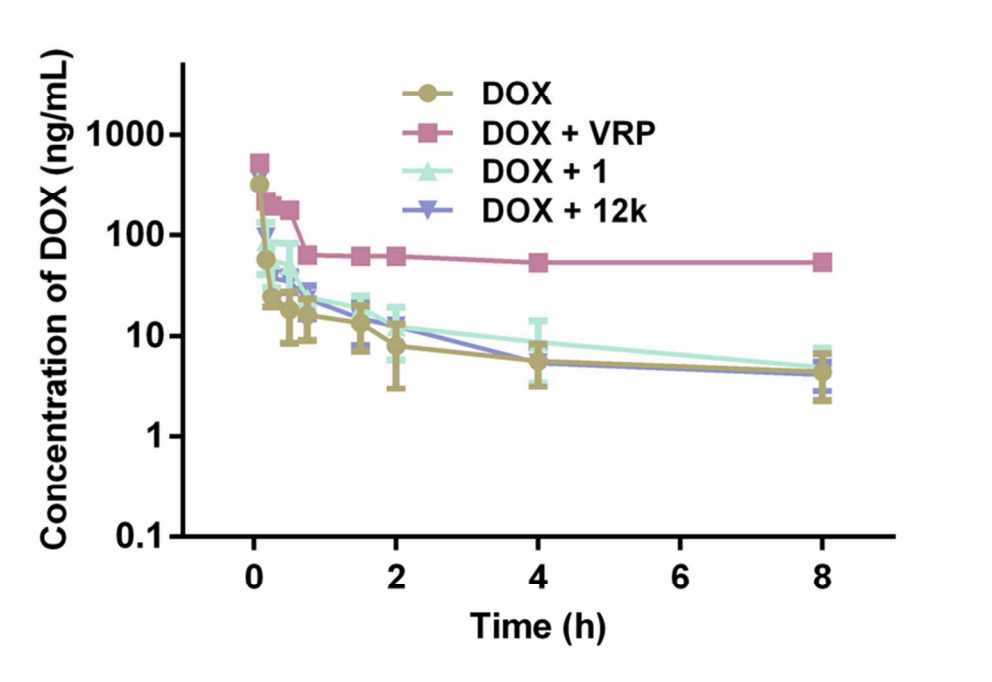

73x50mm (300 x 300 DPI)

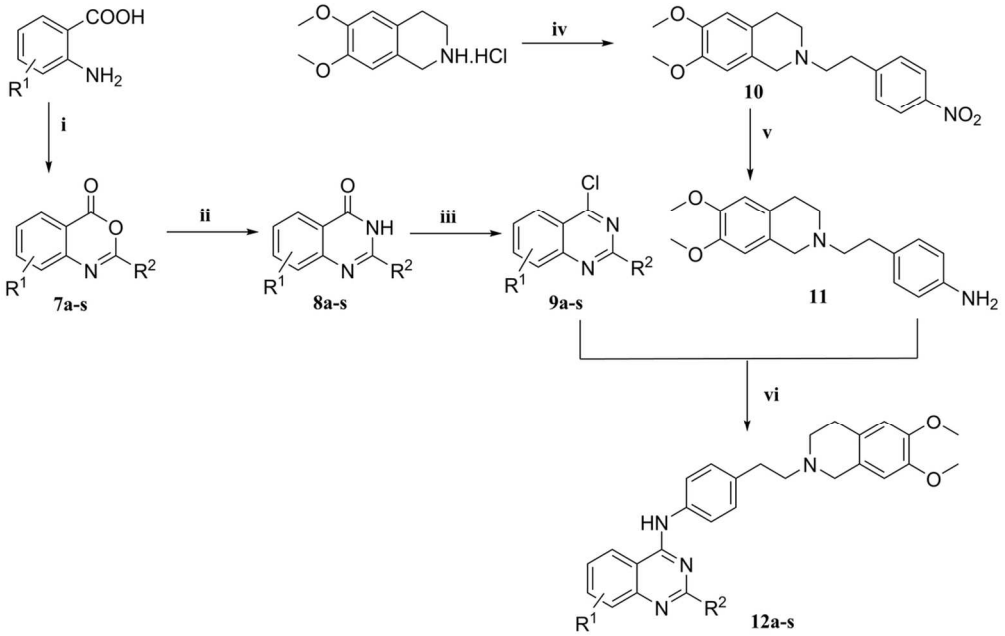

113x72mm (300 x 300 DPI)

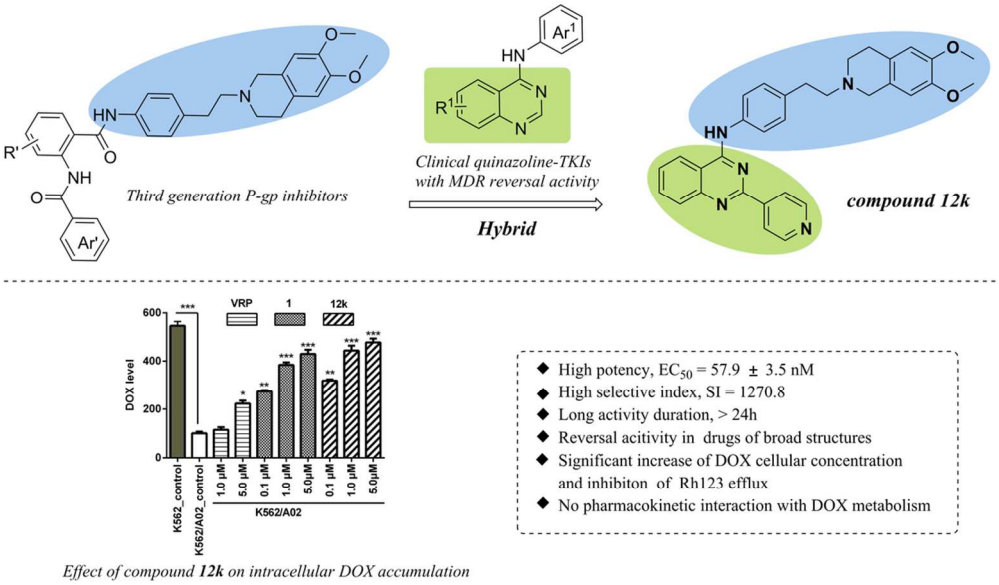

*Effect of compound **12k** on intracellular DOX accumulation*

53x31mm (600 x 600 DPI)